AD_____

Award Number: DAMD17-01-1-0753

TITLE: Investigation of Gene Expression Correlating with Centrosome Amplification in Development and Progression of Breast Cancer

PRINCIPAL INVESTIGATOR: Wilma L. Lingle, Ph.D.

CONTRACTING ORGANIZATION: Mayo Clinic and Foundation, Rochester
Rochester, MN 55905

REPORT DATE: September 2004

TYPE OF REPORT: Annual

PREPARED FOR: U.S. Army Medical Research and Materiel Command
Fort Detrick, Maryland 21702-5012

DISTRIBUTION STATEMENT: Approved for Public Release;
Distribution Unlimited

The views, opinions and/or findings contained in this report are those of the author(s) and should not be construed as an official Department of the Army position, policy or decision unless so designated by other documentation.

REPORT DOCUMENTATION PAGE

Form Approved
OMB No. 074-0188

1. AGENCY USE ONLY (Leave blank)	2. REPORT DATE	3. REPORT TYPE AND DATES COVERED
	September 2004	Annual (15 Aug 2003 - 14 Aug 2004)

4. TITLE AND SUBTITLE
Investigation of Gene Expression Correlating with Centrosome Amplification in Development and Progression of Breast Cancer

5. FUNDING NUMBERS
DAMD17-01-1-0753

6. AUTHOR(S)
Wilma L. Lingle, Ph.D.

7. PERFORMING ORGANIZATION NAME(S) AND ADDRESS(ES)
Mayo Clinic and Foundation, Rochester
Rochester, MN 55905

E-Mail: Lingle.wilma@mayo.edu

8. PERFORMING ORGANIZATION REPORT NUMBER

9. SPONSORING / MONITORING AGENCY NAME(S) AND ADDRESS(ES)
U.S. Army Medical Research and Materiel Command
Fort Detrick, Maryland 21702-5012

10. SPONSORING / MONITORING AGENCY REPORT NUMBER

11. SUPPLEMENTARY NOTES

12a. DISTRIBUTION / AVAILABILITY STATEMENT
Approved for Public Release; Distribution Unlimited

12b. DISTRIBUTION CODE

13. ABSTRACT (Maximum 200 Words)

We previously demonstrated that centrosome amplification correlates with chromosomal instability and loss of differentiation in breast tumors. The goal of this research is to identify genes important in breast cancer due to their association with amplified centrosomes. We determined that centrosomes are amplified prior to invasion and amplification is maintained during progression. We identified candidate genes for further investigation. Last year, we 1) measured chromosomal instability in tumors for which we have gene expression and centrosome amplification data, 2) analyzed the relationships between lymph node and estrogen receptor status, chromosomal instability and centrosome amplification, and 3) developed a collaborative study to look at centrosome amplification, chromosomal instability, and gene expression in a rat model of estrogen-induced mammary cancer. During this last reporting period we 1) demonstrated that expression of Aurora-A, a centrosome-associated kinase, correlates to Nottingham Prognostic Index in human breast tumors, 2) demonstrated that estrogen exposure leads to centrosome amplification and aurora-A over-expression prior to invasion in a rat mammary tumor model, and 3) developed a collaboration to study the effects of cyclin D1 overexpression in a mouse model and demonstrated that cyclin D1 induces centrosome amplification and aneuploidy.

14. SUBJECT TERMS
Centrosome amplification, chromosomal instability, gene expression, Aurora-A, estrogen receptor, cyclin D1

15. NUMBER OF PAGES
69

16. PRICE CODE

17. SECURITY CLASSIFICATION OF REPORT	18. SECURITY CLASSIFICATION OF THIS PAGE	19. SECURITY CLASSIFICATION OF ABSTRACT	20. LIMITATION OF ABSTRACT
Unclassified	Unclassified	Unclassified	Unlimited

Table of Contents

INTRODUCTION

Centrosome amplification is a feature common to many human tumors, including breast, astrocytoma, lung, neuroectodermal tumors, squamous cell carcinomas of the head and neck, and pancreas. Proper structure and function of the duplicated mitotic centrosomes is required for fidelity in chromosome segregation and preservation of diploidy; and proper structure and function of interphase centrosomes is required for maintenance of cell and tissue polarity. We have recently demonstrated that centrosome amplification correlates with chromosomal instability (CIN) and loss of differentiation in breast tumors (Lingle et al., 2002. PNAS 99:1978-1983). The goal of this research is to identify genes that are important in breast cancer due to their association with amplified centrosomes and to initiate investigations of the potential of these genes/proteins as therapeutic targets. This is being accomplished through analysis of gene expression profiles in a series of tumors relative to normal breast tissues. Gene expression profiles are then being correlated with centrosome size for each tissue. Genes whose expression correlates with centrosome size are being studied further. Centrosome and mitotic spindle-associated genes are also being analyzed to identify those with patterns of expression specific for tumor type. In addition, data from the invasive tumors are being analyzed according to estrogen receptor status due to the important influence of ER status on gene expression.

BODY

Task 1. Rank the approximately 50 tumor and 5 normal tissues for which gene expression data will be collected according to centrosome amplification and ploidy. Months 1-7

A. Perform centrosome immunofluorescence on cryosections of the tissues. **Completed.**
B. Quantify centrosome fluorescence signal per cell using scanning laser confocal microscopy analysis. **Completed.**
C. Rank tumors according to their degree of centrosome amplification. **Completed.**
D. Determine tumor ploidy by ~~flow cytometry and~~ FISH analysis. **Completed in previous year.**

Results from Tasks 1A-C were published in PNAS (Lingle et al., 2002). The publication was appended to the 2003 report. Results from Task 1D were presented in the 2004 report. Briefly, those data indicated that ER negative tumors have higher CIN and more centrosomes than ER positive tumors. The correlation coefficients of centrosome size and number with measures of chromosomal instability were also presented in the 2003 report. Highly significant correlation in LN- and ER- tumors of centrosome amplification with number of clones, number of karyotypes, CIN, and chromosomal gains. **These results provide evidence of fundamental differences in the relationship between centrosome amplification and chromosomal instability in tumors based on ER status and LN status.**

Task 2. Select cDNA sequences whose expression is positively correlated to centrosome amplification and those associated with aggressive tumors. Months 7-8

A. Determine the correlation coefficient of sequence expression relative to centrosome amplification in aneuploid compared to diploid tumors. **Completed.**
B. Select sequences with strong positive expression coefficients only in aneuploid tumors and associated with aggressive tumors. **Completed.**

C. Begin manuscript preparation describing the sequences selected by this method. **Not yet begun.**

Task 3. Identify and analyze the cDNA sequences selected in Task 2. Months 9-15

A. Divide selected sequences into groups as follows:
   I. known genes encoding characterized proteins
   II. known genes or unigenes encoding uncharacterized or poorly characterized proteins
   III. ESTs with no known gene homology **Completed.**
B. Search the Unigene database for genes and unigenes with homologies to the Group III ESTs. **Ongoing**.
C. Characterize genes in Group II for structural motifs and functional domains that may place then in families of characterized genes. **Ongoing.**
D. Preparation of manuscript describing the sequences identified. **First manuscript published (see Appendix A).**

Gene Groups I-III for genes whose expression correlates with centrosome size in ER- tumors were presented in the 2003 report. Group I contains 22 genes, 11 of which have a positive correlation and 9 of which have a negative correlation. Seven of the 22 genes are involved in gene expression or chromosome replication and nine genes are involved in cell cycle. Group II contains eleven genes, four of which have a positive correlation and seven of which have a negative correlation. Group III contains 14 sequences about which very little is known. Nine of the genes have a positive correlation and five have a negative correlation. We continue to update the genes in Groups II and III through the NCBI unigene portal and are also investigating genes known to be associated with centrosome structure and function. **A manuscript describing one analysis of the gene expression studies has been published (Miller et al., 2004, Appendix A). This analysis demonstrated that expression levels of the centrosome-associated kinase aurora-A (also known as STK6 and STK15) correlate with Nottingham Prognostic Index in the patient cohort.** We will continue to work with aurora-A as described in Task 4. Cyclin D1 and TTK (also known as MPS1) have also been selected for investigation as described in Task 4 based on their known effects on centrosomes. Cyclin D also has oncogenic activity. We have selected 2 genes to investigate based on the correlation of their expression levels to centrosome size in ER negative tumors; the erythropoietin receptor (90% positive correlation coefficient) and DAXX: death-associated protein 6 (92% negative correlation coefficient). There is evidence that the erythropoietin receptor contributes to the survival of cancer cells and has functional significance in breast cancers.

Task 4. Investigation of the biological significance of genes prioritized from Task 3 by correlating gene over-expression with phenotypic data. Months 12-36. **In progress (please see proposed change in task timeline below).**

A. Insert genes into expression vector driven by the CMV promoter for transfection into hTERT-transfected normal mammary epithelial cells and quantify expression levels. *We have altered our research plan to use adenoviral vectors and tetracyclin-inducible vectors for some of these studies.*
B. Collect phenotypic information from transfected cells, including changes in centrosome structure and function, alterations in karyotype, formation of abnormal mitotic spindles, and altered response to ionizing radiation.
C. Preparation of manuscripts with data on biological significance of the chosen sequences.

We have shown that aurora-A expression levels increase at the same time centrosome amplification is evident in hyperplastic lesions that precede invasive ductal carcinoma in an estrogen-induced rat model of mammary cancer (Li et al., 2004, Appendix C). We will continue to explore the role of aurora-A in centrosome function and carcinogenesis in over-expression studies in cell lines.

Using adenoviral vectors, we showed that short-term over-expression of cyclin D1 in immortalized hMECs resulted in the formation of multipolar mitotic spindles and abnormal centrosomes in less than 48 hours (Nelsen et al., 2004, Appendix D). We will continue these experiments in the hMEC lines.

Proposed change in task timeline.

In last year's report, we described a new commercial system, Nucleofector (AMAXA, GmbH), that utilizes electroporation under defined conditions in the presence of specifically tailored buffers and reagents for delivering expression constructs to our cultured cells. We have optimized this system for our cells and are now able to achieve useful delivery efficiencies of between 70-90%, compared to our previous methods with less than 5% efficiency. We are using this system to deliver expression vectors to our cell lines and also to establish a tetracycline-on inducible hTERT hMEC cell line for the proposed experiments. This inducible cell line will allow us to easily observe early changes induced by expression of genes we have identified during the course of this research project. The inducible system will be especially important to investigate changes that occur in soon after gene expression is altered. We requested, and were granted, a no cost extension for this project in order to complete Task 4.

KEY RESEARCH ACCOMPLISHMENTS

- Demonstrated that expression of Aurora-A, a centrosome-associated kinase, correlates to Nottingham Prognostic Index in human breast tumors (see publication #1 below).
- Demonstrated that estrogen exposure leads to centrosome amplification and aurora-A over-expression prior to invasion in a rat mammary tumor model (see publication #3 below).
- Developed a collaboration to study the effects of cyclin D1 over-expression in a mouse model and demonstrated that cyclin D1 induces centrosome amplification and aneuploidy (see publication # 4 below).

REPORTABLE OUTCOMES

PUBLICATIONS

1. Miller, DV. Leontovich, AA. **Lingle, WL**. Suman, VJ. Mertens, ML. Lillie, J. Ingalls, KA. Perez, EA. Ingle, JN. Couch, FJ. Visscher, DW. 2004. Utilizing Nottingham Prognostic Index in microarray gene expression profiling of breast carcinomas. Modern Pathology. 17(7):756-64.
2. Salisbury, JL, D'Assoro, A, **Lingle, WL**. Centrosome Amplification and The Origin of Chromosomal Instability in Breast Cancer. 2004. Journal of Mammary Gland Biology and Neoplasia. 9(3):275-283.
3. Li, JJ, Weroha, SJ, **Lingle, WL**, Papa, D, Salisbury, JL, and Li, SA. 2004. Estrogen Mediates Aurora-A Overexpression, Centrosome Amplification, Chromosomal Instability,

and Breast Cancer in Female ACI Rats. PNAS. In press (Dec 24, 2004 on-line publication date).
4. Nelsen, CJ, Kuriyama, R, Hirsch, B, Negron, VC, **Lingle, WL**, Goggin, MM, Stanley, MW, and Albrecht, JH. 2004. Short-term cyclin D1 overexpression induces centrosome amplification, mitotic spindle abnormalities, and aneuploidy. JBC. In Press (Oct 26, 2004 on-line publication date).

CONCLUSIONS

The results from this research continue to support the hypothesis that centrosome amplification can be used to identify a subset of genes involved in the development and progression of cancer. We have demonstrated that estrogen receptor status is an especially critical factor to include in the interpretation of these data, and have demonstrated this in a rat model of estrogen induced mammary tumors.

APPENDICES

A. Miller, DV. Leontovich, AA. **Lingle, WL**. Suman, VJ. Mertens, ML. Lillie, J. Ingalls, KA. Perez, EA. Ingle, JN. Couch, FJ. Visscher, DW. 2004. Utilizing Nottingham Prognostic Index in microarray gene expression profiling of breast carcinomas. Modern Pathology. 17(7):756-64.
B. Salisbury, JL, D'Assoro, A, **Lingle, WL**. Centrosome Amplification and The Origin of Chromosomal Instability in Breast Cancer. 2004. Journal of Mammary Gland Biology and Neoplasia. 9(3):275-283.
C. Li, JJ, Weroha, SJ, **Lingle, WL**, Papa, D, Salisbury, JL, and Li, SA. 2004. Estrogen Mediates Aurora-A Overexpression, Centrosome Amplification, Chromosomal Instability, and Breast Cancer in Female ACI Rats. PNAS. In press (Dec 24, 2004 on-line publication date).
D. Nelsen, CJ, Kuriyama, R, Hirsch, B, Negron, VC, **Lingle, WL**, Goggin, MM, Stanley, MW, and Albrecht, JH. 2004. Short-term cyclin D1 overexpression induces centrosome amplification, mitotic spindle abnormalities, and aneuploidy. JBC. In Press (Oct 26, 2004 on-line publication date).

Modern Pathology (2004) 17, 756–764

www.modernpathology.org

Utilizing Nottingham Prognostic Index in microarray gene expression profiling of breast carcinomas

Dylan V Miller[1], Alexey A Leontovich[2], Wilma L Lingle[2], Vera J Suman[3], Maureen L Mertens[4], James Lillie[4], Kimberly A Ingalls[4], Edith A Perez[5], James N Ingle[6], Fergus J Couch[2] and Daniel W Visscher[1]

[1]*Department of Anatomic Pathology;* [2]*Department of Experimental Pathology;* [3]*Department of Biostatistics, Mayo Clinic, Rochester, MN, USA;* [4]*Millenium Pharmaceuticals, Inc., Cambridge, MA, USA;* [5]*Department of Hematology/Oncology, Mayo Clinic, Jacksonville, FL, USA and* [6]*Department of Oncology, Mayo Clinic, Rochester, MN, USA*

We report a novel approach to gene expression profiling using the Nottingham Prognostic Index (NPI) to stratify 26 patients with invasive breast carcinoma. As an aggregate index of parameters reflecting metastatic potential, growth rate, and genetic instability the NPI has distinct advantages over other clinicopathologic features used to segregate breast cancer patients. As a continuous variable it offers a responsive and sensitive means of modeling a continuum of clinical aggressiveness. Using RNA extracted from 26 tumors and cDNA microarrays with 23 343 unique genetic elements, 84 genes and expressed sequence tags were identified whose expression patterns correlated with NPI. Differential expression by immunohistochemistry (IHC) was also observed for two of three genes evaluated by this method. Correlation was determined by the Spearman rank correlation method with null distribution analysis. Among the 84 genetic elements were seven previously implicated in neoplastic progression (including the two demonstrating differential expression by IHC), 11 without specific cancer association but localized to chromosomal sites whose loss or gain has been identified in cytogenetic studies of breast carcinoma, and 73 not previously associated with breast carcinoma. Collectively, the expression patterns of these 84 elements have potential to distinguish high and low NPI patient samples. These data add support to the assertion that prognostic groups of breast carcinoma are reflected in distinguishable expression profiles of a limited set of genes.
Modern Pathology (2004) **17,** 756–764, advance online publication, 9 April 2004; doi:10.1038/modpathol.3800114

Keywords: breast neoplasms; carcinoma, infiltrating duct; Nottingham Prognostic Index; gene expression profiling; cDNA microarray

The specific molecular events contributing to the spectrum of clinical aggressiveness and therapeutic responsiveness in breast carcinoma are poorly understood, but are thought to involve multifactorial, interactive, and stepwise alterations of gene expression.

The current ability of grade and stage to assess prognosis and predict therapeutic response is less than ideal. Up to one-third of women with negative axillary lymph nodes will experience recurrence and approximately one-third of node-positive patients not receiving adjuvant therapy will be recurrence free after 10 years.[1,2] Consideration of other factors such as special histologic type, hormone and growth factor receptor expression, and other individual parameters marginally improve this ability,[3,4] but likely represent only a fraction of the molecular mechanisms ultimately determining the clinical behavior of tumors.

Analyzing the variation in aggregate gene expression using gene array technology offers a powerful approach that has been employed in identifying molecular markers important in predicting outcome as well as response to targeted therapy. The ultimate aims of such endeavors may be to characterize conserved 'molecular signatures' that more accurately predict prognosis, or to characterize novel molecular mechanisms of malignant transformation and cell growth and thereby

Correspondence: DW Visscher, MD, Department of Laboratory Medicine and Pathology, Mayo Clinic, Hilton 11, Rochester, MN, 55906, USA.
E-mail: visscher.daniel@mayo.edu
Received 24 September 2003; revised 17 February 2004; accepted 18 February 2004; published online 9 April 2004

potential avenues for targeted pharmacotherapeutic modalities.[5]

Several recent studies have used factors such as axillary lymph node metastasis, local recurrence, distant metastasis, outcome, hormone receptor expression, and BRCA1/BRCA2 mutations to identify molecular signatures of clinical relevance.[6–14] These factors have the advantage of being unequivocal, easily ascertained, and clinically practical. However, complex statistical algorithms must be employed to correlate the continuous variable data from gene expression microarrays with the binary or discrete variable data of the other factors.

The Nottingham Prognostic Index (NPI) was derived from tumor registry data as a robust means for predicting outcomes in breast cancer patients.[15] Despite some significant limitations—namely unproven applicability in the era of mammographically detected lesions and lack of resolution in predicting behavior of tumors less than 1.0 cm[16,17]—it has been validated independently[18–20] and prospectively[21] as a means of segregating patients into excellent, good, moderate, and poor prognosis groups. Unlike nodal status, hormone receptor expression, grade, and other binary measures previously used in stratifying cases for gene expression profiling, the NPI is a continuous variable. As such, it allows for more straightforward correlation analysis.

We report the results of our gene expression profiling of 26 patients with invasive ductal carcinoma employing direct correlation analysis between NPI scores and the raw expression data of 23 343 genes and expressed sequence tags (EST).

Materials and methods

Institutional Review Board approval for this study was obtained at our institution before commencing. Pathology reports and histologic sections from 26 patients with invasive ductal carcinoma undergoing surgery at the Mayo Clinic between 1997 and 2000 were reviewed to determine the NPI for each case using the formula put forth by the Nottingham group[15,22] with the modification of lymph node scoring proposed by the Swedish Breast Cancer Cooperative Group.[23] In short, the index is a sum of three separate scores: grade (scored as 1, 2, or 3 — using the three-tiered Nottingham scale), size (score obtained by multiplying the size in cm by 0.2), and lymph node status (scored as: no lymph metastasis = 1, 1–4 involved lymph nodes = 2, and >4 involved lymph nodes = 3).

RNA was extracted from fresh frozen tissue obtained at the time of surgery for 26 patients as well as five normal control and seven patients with ductal carcinoma *in situ* (DCIS) (three low-grade DCIS and four high-grade DCIS). Tissue samples were snap frozen in the frozen section laboratory. Cryostat sections of each sample were examined to ensure the invasive and intraductal carcinoma specimens contained at least 75% tumor and for verification of the normal control specimens. Total RNA was extracted from 10 to 15, 10 μm frozen tissue sections of each sample. The quantity of RNA was determined by OD_{260} spectrophotometry and the quality was assessed by agarose gel electrophoresis.

Expression profiling for all 38 patient RNA samples was performed at Millennium Pharmaceuticals, LLC (Cambridge, MA, USA) using an automated high throughput cDNA microarray assay comprised of 30 512 unique cDNAs including 5111 well-characterized genes and 18 232 ESTs, or Unigene sequences (Research Genetics, Inc., Huntsville, AL, USA).

Correlation analysis using the Spearman rank correlation coefficient determination was performed by comparing the NPI values for the invasive carcinoma patients to the raw microarray expression data. The null distribution of the Spearman correlation was determined to assess the number of chance random correlations anticipated. Genes for which the absolute value of the Spearman rank correlation coefficient was greater than 0.6 were considered significantly associated with NPI. The expression data of selected genes, in the invasive carcinoma cohort as well as the control and DCIS groups, were normalized by mean centering and represented graphically using the TreeView software program (Stanford Univeristy, Palo Alto, CA, USA).

Gene attributes, including known or potential cancer association, were ascertained using the Unigene, LocusLink, and OMIM databases available from the National Center for Biotechnology Information (http://ncbi.nlm.nih.gov).

Immunoperoxidase staining of frozen tissue sections (from the same tissue from which RNA was extracted) was performed using commercially available monoclonal antibodies (Santa Cruz Biotechnology, Inc., Santa Cruz, CA, USA) directed against protein products of the cancer-associated genes identified by the correlation analysis above. Slides were processed on a Ventana ES (Ventana Medical Systems Inc., Tucson, AZ, USA) autostainer (dilutions provided below) that utilized labeled streptavidin biotin detection chemistry with 5-aminoethyl-carboxazole as the chromogen. Tumor sections were examined in a blinded fashion and staining of the benign or neoplastic epithelial cells was scored on a scale of 0–4+. The cellular staining pattern (nuclear, cytoplasmic, membrane, etc) observed in the invasive tumor, benign, and stromal cells was noted for each case. Correlation between the raw microarray gene expression data and the immunohistochemical expression data were determined using the Spearman rank methodology.

Results

Demographic and clinical parameters of the patients and tumors are summarized in Table 1 and Figure 1.

Table 1 Patient and tumor parameters

Gender (M:F)	(1:25)
Median age (range)	65 (29–90)
Mean tumor size (range)	2.5 (1.1–5.0)
Lymph node metastases:	
0	12
1–4	7
>4	7
Histologic grade	
I	4
II	11
III	11
Mean NPI (range)	4.6 (2.4–6.8)

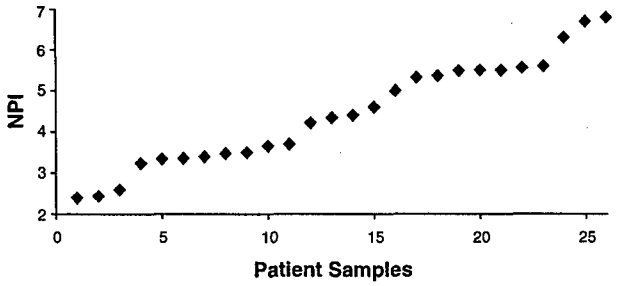

Figure 1 NPI distribution for 26 patients with invasive breast carcinoma. Patient samples listed in order of increasing NPI. (NPI: Nottingham Prognostic Index)

A total of 124 array positions representing 50 well-characterized genes and 34 ESTs demonstrated substantial positive or negative correlation with NPI ($|r| > 0.6$). Supervised clustering of the microarray showed low expression values gradually merging into high expression values with increasing NPI in the positive correlation gene group and the opposite pattern in the negative correlation gene group (Figure 2).

Of the 46 genes/ESTs for which expression correlated well with increasing NPI ($r > 0.6$), 35 did not show increased expression in normal controls, 41 had no increase in expression in low-grade DCIS, and 36 had no increase in high-grade DCIS. Of the 38 genes/ESTs for which decreased expression correlated well with increasing NPI ($r < -0.6$), 29 also showed increased expression in the normal controls, 31 had increased expression in low-grade DCIS, and 34 were increased in high grade DCIS.

Using the null distribution of the Spearman correlations for 26 patients, 30 512 array positions, and $|r| > 0.6$, an estimated 0.13% (or 39) of the array positions would be expected to show random correlation.

Among those genes overexpressed in tumors with higher NPI scores, were two previously associated with malignant transformation: tumor protein D52 like protein 2 (TPD52L2),[24] and serine-threonine kinase 6 (STK6).[25] Among those genes expressed at increased levels in tumors with lower NPI scores, as well as normal controls, were four whose reduced expression has been implicated in neoplastic progression (mothers against decapentaplegic homolog 4 (MADH4),[26] p53 inducible protein 1 (TP53Inp1),[27] dual specificity phosphatase 5 (DUSP5),[28] GATA sequence binding protein 3 (GATA3),[29] and tumor rejection antigen 1 (TRA1)).[30]

Commercially available monoclonal antibodies suitable for use in frozen section immunohistochemistry (IHC) were obtained for three of the seven cancer-associated genes: GATA3 (clone HG3-31, 1:100 dilution), MADH4 (clone B-8, 1:50 dilution), and TRA1 (clone C-19, 1:100 dilution) (Santa Cruz Biotechnology, Inc., Santa Cruz, CA, USA). Immunoperoxidase staining was performed on three normal control and 17 tumor samples (there was insufficient frozen tissue for the testing of the remaining samples). IHC expression of MADH4 and GATA3 showed statistically significant correlation with the raw microarray expression data (Figure 3). Staining for MADH4 was characterized by a cytoplasmic pattern of expression that was strongest in the benign and low NPI tumors. Staining for GATA3 was predominantly nuclear in pattern with the strongest intensity seen low NPI tumors. Less intense staining was observed in benign controls as well as high NPI tumors. Staining for TRA1 did not correlate with microarray expression values. The TRA1 pattern of staining was cytoplasmic and predominantly within stromal cells; the epithelial component stained negatively or equivocally (1+) (Figure 4).

In addition to specific cancer-associated genes, disproportionate increases or decreases of multiple separate genes/ESTs at certain chromosomal regions associated with loss or gain in breast tumors were noted in tumors with higher NPI scores. Increased expression was observed in genes/ESTs localized to 1q21, 6p21, 7p14, 11q13–23, and 20q13. Decreased expression was seen in genes/ESTs localized to 1q23–25, 9q33–34, 10q25–26, 17p11–13, 18q12–21, and 19q11–13 (Table 2).

Discussion

The specific genetic elements (or combination thereof) contributing to the spectrum of clinical aggressiveness and therapeutic responsiveness seen in breast carcinomas are poorly understood. These are likely multifactorial, interactive, and stepwise alterations of expression that continue to evolve even after a tumor becomes invasive. As an aggregate index comprised of parameters reflecting metastatic behavior, growth rate and genetic instability, the NPI has several distinct advantages over other clinicopathologic features used to segregate breast cancer patients in gene expression profiling studies. The NPI is thus able to reflect and model tumor progression by assigning a numeric value to tumors approximating different points along a continuum of clinical aggressiveness.

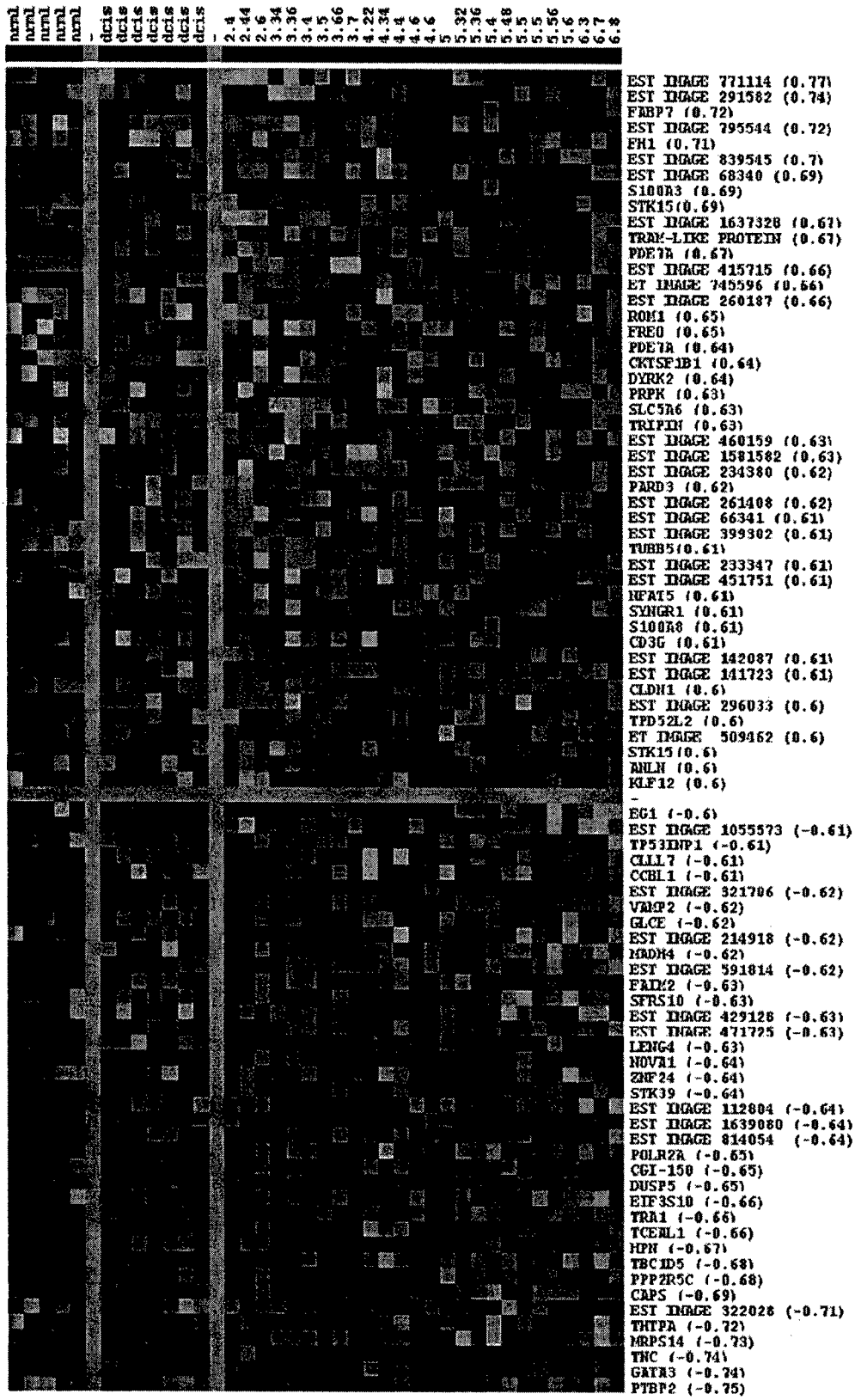

Figure 2 Supervised clustering of microarray data for selected genes. The patient samples are arranged in columns. The invasive carcinoma patients are in order of increasing NPI. Gene/ESTs comprise the rows. The HUGO Gene Nomenclature Committee designation is used for genes and the IMAGE database identifier is given for the ESTs. The Spearman rank correlation coefficient for each gene/EST follows in parentheses.

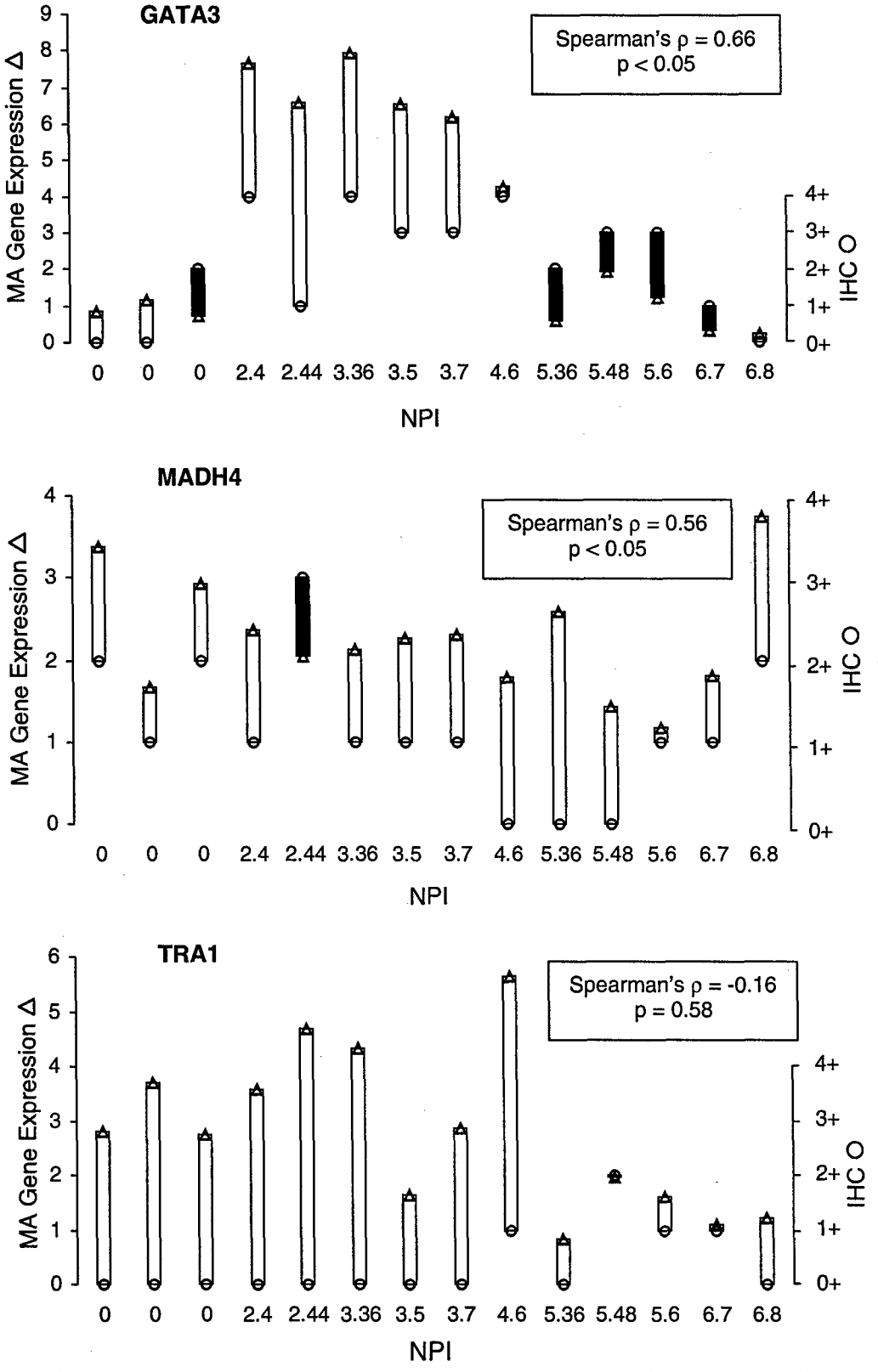

Figure 3 Differential expression of GATA3, MADH4, and TRA1 by immunohistochemistry and microarray. Line drop scatter plots of the microarray (MA) gene expression and IHC expression values for three cancer-associated genes identified in this study. MA (Δ) values are expressed as dimensionless relative units (fold difference). IHC values (○) are the tumor cell staining score. White bars between points indicate a positive difference between MA and IHC values, dark bars indicate a negative difference. Spearman rank ρ and P values are given for each gene.

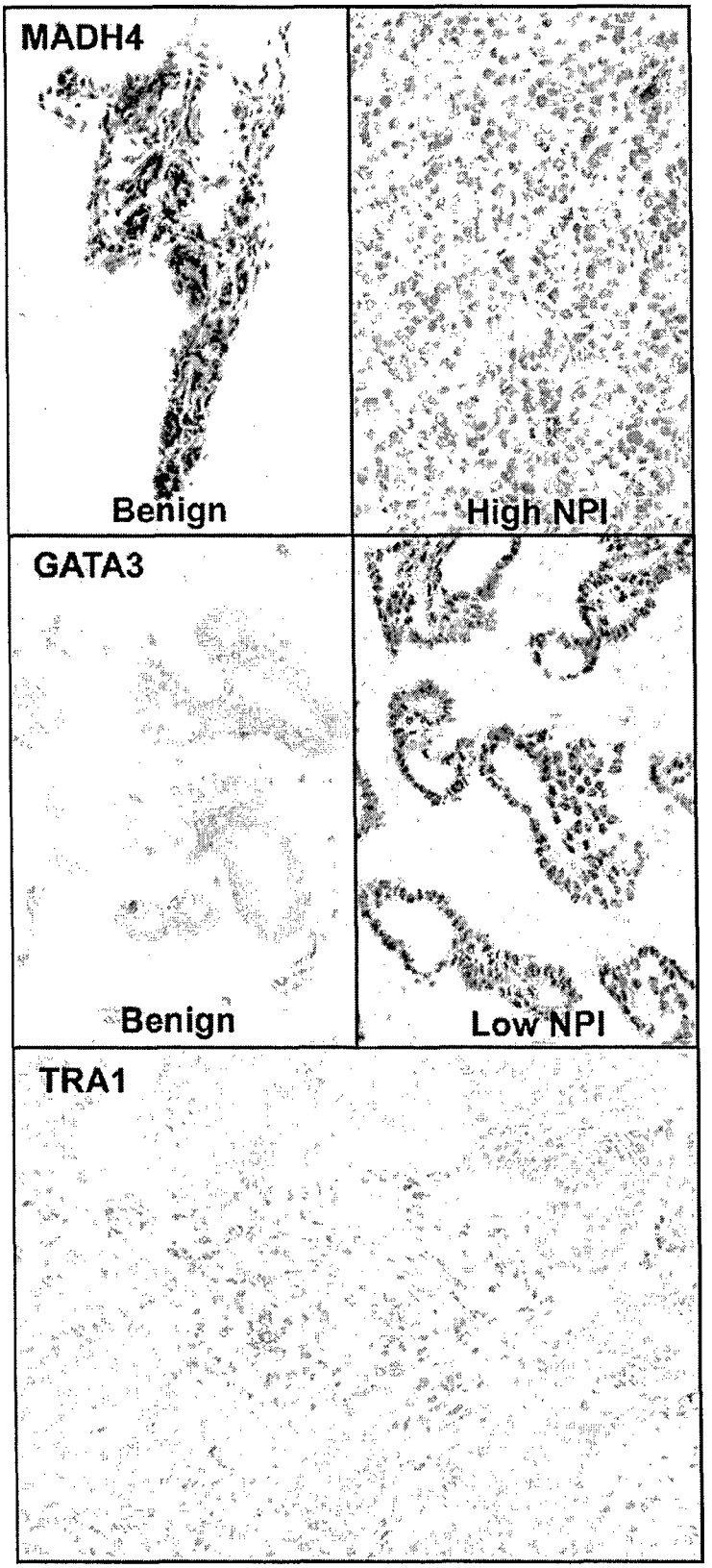

Figure 4 MADH4, GATA3, and TRA1 immunohistochemistry. Representative photomicrographs (× 200) of immunoperoxidase-stained frozen tissue sections using antibodies directed against MADH4, GATA3, and TRA1.

Table 2 Differential expression at specific chromosomal sites

Genes/ESTs	*Locus*	*r*	*Reported frequency*
Gains			
S100A3	1q21	0.61	61%[35]
S100A8	1q21	0.69	
EST IMAGE 84820	6p21.1	0.67	Reported but frequency not stated[36]
TUBB5	6p21.31	0.61	
ANLN	7p14–15	0.60	44%[35]
EST IMAGE 771114	7p14.3	0.77	
ROM1	11q13	0.66	38%[37] [11% High Level Amplification at 11q23][35]
CD3G	11q23	0.61	
TPD52L2	20q13.2	0.60	55% [11% High Level Amplification at 20q13.2][35]
STK6	20q13.2	0.69	
Losses			
MRPS14	1q23–25	−0.73	65% [1q21-23 commonly deleted][38,39]
EST IMAGE 814054	1q24–25	−0.64	
TNC	9q33	−0.74	39% [9q33 commonly deleted][40]
CCBL1	9q34.13	−0.61	
DUSP5	10q25	−0.65	30%[35]
EIF3S10	10q26	−0.66	
EST IMAGE 591814	17p11.1	−0.62	30%[41]
POLR2A	17p13.1	−0.65	
CGI-150	17p13.3	−0.65	
VAMP2	17p31.1	−0.62	
MADH4	18q21	−0.64	58%[35]
ZNF24	18q12	−0.62	
HPN	19q11–13.2	−0.67	Reported but frequency not stated[43]
LENG4	19q13.3	−0.63	

While no genetic elements with perfect correlation between expression and NPI were identified, two well-characterized genes associated with malignancy were increasingly overexpressed with increasing NPI scores. STK6 (also known as STK15, BTAK, or aurora2) overexpression has been implicated in centrosome abnormalities and aneuploidy in p53 deficient cultured cell lines.[25] More specifically, STK6 has been described as amplified in up to 12% of breast tumors, and overexpressed in substantial percentage of the nonamplified cases.[31] TPD52L2 is another less well-characterized putative oncogene.[24]

In addition, five genes whose reduced expression has been implicated in malignant transformation (ie putative tumor suppressor genes) were expressed at relatively increased levels in patients with lower NPI scores as well as in DCIS and normal controls. MADH4 (or SMAD4 or DPC4) loss has been well described in pancreatic and juvenile polyposis associated colorectal tumors,[26,32] TP53Inp1 is thought to participate in p53 mediated 'gatekeeper' functions,[27] GATA3 interacts with TGF-β mediated pathways of tumor suppression and has been shown to be coexpressed with estrogen receptor,[29,33,34] (Reinholz M and Lingle W, Unpublished Data, 2004.) DUSP5 inhibits the MAP kinase pathway of cell proliferation signaling,[28] and TRA1 (GRP94, or GP96) also seems to impart a protective effect from malignant transformation.[30]

Other genes/ESTs such as POLR2A (an RNA polymerase) and TUBB5 (a member of the beta tubulin family) may reflect proliferation-related increases in metabolic, protein synthetic, or cytoskeletal restructuring activity. The sporadically increased expression of some of these genes in the normal controls may similarly reflect transient homeostatic changes. Still other markers such as FABP7 (a fatty acid binding protein expressed in adipocytes) may represent benign cellular constituents disproportionately present in either higher or lower NPI score samples.

Differential expression by IHC correlated with the microarray expression values for two of the three genes (GATA3 and MADH4) examined in our study. A third marker (TRA1) showed sporadic expression by IHC, predominantly within stromal cells, that did not correlate with expression data for TRA1 in the microarray. This likely represents a disproportion of non-neoplastic stromal elements within the samples, a recognized susceptibility of this technique.

In addition to specific cancer-associated genes, multiple separate genes/ESTs localized to specific chromosomal regions showed increased or decreased expression in the high NPI patient samples. These might indirectly represent deletions or amplifications of these regions, the majority of which have been observed previously in cytogenetic analyses of breast carcinoma. Specifically, the apparent gains at 1q21, 20q13.2, and 7p14 and the apparent losses at 1q23–25 and 9q33 match

those most consistently and frequently reported in the literature.

Our data suggest that prognostic groups of breast carcinomas can be defined by distinguishable expression profiles of a limited set of genes ($n = 84$). These data are similar to those of van de Vijver *et al*,[10] who demonstrated a significant correlation between outcome and expression of 70 genes identified by expression array technology, and actually improved prognostic discrimination using that gene profile instead of NIH or St Gallen's prognostic criteria. From a biological standpoint, these data are important in the sense of demonstrating that the spectrum of genetic alterations corresponding to clinical aggressiveness in malignant neoplasms is not random. Rather, it is potentially definable using a finite number of variables. From a prognostic standpoint, careful studies will be required to determine whether our gene expression profiles can improve outcome prediction beyond the resolution of NPI in a larger group of patients. From the standpoint of target discovery, our findings lend support to several recent reports of novel genes important in the breast neoplasia and point in new directions to genes and markers warranting further exploration.

Acknowledgements

We thank Dirk Larson, Diane Grill and Ann Oberg, PhD of the Biostatistics Department and Center for Patient Oriented Research of Mayo Clinic—Rochester for their assistance with Spearman's rank correlation and null distribution statistical analysis. Supported by a grant from the Breast Cancer Research Foundation (WLL, ALL, and EAP). Microarray hybridization was performed by Millennium Pharmaceuticals, Inc. at their cost (JL, MLM, KAI).

References

1 Early Breast Cancer Trialists' Collaborative Group. Polychemotherapy for early breast cancer: an overview of the randomised trials. Lancet 1998;352:930–942.
2 Early Breast Cancer Trialists' Collaborative Group. Tamoxifen for early breast cancer: an overview of the randomised trials. Lancet 1998;351:1451–1467.
3 Isaccs C, Stearns V, Hayes DF. New prognostic factors for breast cancer recurrence. Semin Oncol 2001;28: 53–67.
4 Anderson TJ, Alexander FE, Lamb J, *et al*. Pathology characteristics that optimize outcome prediction of a breast screening trial. Br J Cancer 2000;83:487–492.
5 Ochs MF, Godwin AK. Microarrays in cancer: research and applications. Biotechniques 2003;34:S4–S15.
6 Perou CM, Sorlie T, Eisen MB, *et al*. Molecular portraits of human breast tumours. Nature 2000;406: 747–752.
7 Sorlie T, Perou CM, Tibshirani R, *et al*. Gene expression patterns of breast carcinomas distinguish tumor subclasses with clinical implications. Proc Natl Acad Sci USA 2001;98:10869–10874.
8 Hedenfalk I, Duggan D, Chen Y, *et al*. Gene-expression profiles in hereditary breast cancer. N Engl J Med 2001;344:539–548.
9 van't Veer LJ, Dai H, van de Vijver MJ, *et al*. Gene expression profiling predicts clinical outcome of breast cancer. Nature 2002;415:530–536.
10 van de Vijver MJ, He YD, van't Veer LJ, *et al*. A gene-expression signature as a predictor of survival in breast cancer. N Engl J Med 2002;347:1999–2009.
11 Gruvberger S, Ringner M, Chen Y, *et al*. Estrogen receptor status in breast cancer is associated with remarkably distinct gene expression patterns. Cancer Res 2001;61:5979–5984.
12 West M, Blanchette C, Dressman H, *et al*. Predicting the clinical status of human breast cancer by using gene expression profiles. Proc Natl Acad Sci USA 2001;98:11462–11467.
13 van't Veer LJ, Dai H, van de Vijver MJ, *et al*. Expression profiling predicts outcome in breast cancer (Letter). Breast Cancer Res 2002;5:57–58.
14 Ahr A, Holtrich U, Solbach C, *et al*. Molecular classification of breast cancer by gene expression profiling. J Pathol 2001;195:312.
15 Galea MH, Blamey RW, Elston CE, *et al*. The Nottingham Prognostic Index in primary breast cancer. Breast Cancer Res Treat 1992;22:207–219.
16 Anderson TJ. Breast cancer prognostication in the 21st century and the Nottingham prognostic index (Editorial). J Clin Pathol 2002;55:86–87.
17 Cserni G. The effect of sentinel lymph node biopsy on the Nottingham Prognostic Index in breast cancer patients. J R Coll Surg Edinburg 2001;46:208–212.
18 Balslev I, Axelsson CK, Zedeler K, *et al*. The Nottingham Prognostic Index applied to 9,149 patients from the studies of the Danish Breast Cancer Cooperative Group (DBCG). Breast Cancer Res Treat 1994;32: 281–290.
19 D'Eredita G, Giardina C, Martellotta M, *et al*. Prognostic factors in breast cancer: the predictive value of the Nottingham Prognostic Index in patients with a long-term follow-up that were treated in a single institution. Eur J Cancer 2001;37:591–596.
20 Sundquist M, Thorstenson S, Brudin L, *et al*. Applying the Nottingham Prognostic Index to a Swedish breast cancer population. South East Swedish Breast Cancer Study Group.. Breast Cancer Res Treat 1999;53:1–8.
21 Robertson JF, Dixon AR, Nicholson RI, *et al*. Confirmation of a prognostic index for patients with metastatic breast cancer treated by endocrine therapy. Breast Cancer Res Treat 1992;22:221–227.
22 Elston CW, Ellis IO. Pathological prognostic factors in breast cancer. I. The value of histologic grade in breast cancer: experience from a large study with long term follow-up. Histopathology 1991;19:403–410.
23 Swedish Breast Cancer Cooperative Group. Randomized trial of two versus five years of adjuvant tamoxifen for postmenopausal early stage breast cancer. J Natl Cancer Inst 1996;88:1543–1549.
24 Nourse CR, Mattei MG, Gunning P, *et al*. Cloning of a third member of the D52 gene family indicates alternative coding sequence usage in D52-like transcripts. Biochim Biophys Acta 1998;1443: 155–168.
25 Meraldi P, Honda R, Nigg EA. Aurora-A overexpression reveals tetraploidization as a major route to

centrosome amplification in p53−/− cells. EMBO J 2002;21:483–492.
26 Hahn SA, Schutte M, Hoque AT, *et al.* DPC4, a candidate tumor suppressor gene at human chromosome 18q21.1. Science 1996;271:350–353.
27 Okamura S, Arakawa H, Tanaka T, *et al.* p53DINP1, a p53-inducible gene, regulates p53-dependent apoptosis. Mol Cell 2001;8:85–94.
28 Kovanen PE, Rosenwald A, Fu J, *et al.* Analysis of gamma c-Family Cytokine Target Genes. Identification of dual-specificity phosphatase 5 (DUSP5) as a regulator of mitogen-activated protein kinase activity in interleukin-2 signaling. J Biol Chem 2003;278: 5205–5213.
29 Blokzijl A, ten Dijke P, Ibanez CF. Physical and functional interaction between GATA-3 and Smad3 allows TGF-beta regulation of GATA target genes. Curr Biol 2002;12:35–45.
30 Maki RG, Old LJ, Srivastava PK. Human homologue of murine tumor rejection antigen gp96: 5′-regulatory and coding regions and relationship to stress-induced proteins. Proc Natl Acad Sci USA 1990;87:5658–5662.
31 Zhou H, Kuang J, Zhong L, *et al.* Tumour amplified kinase STK15/BTAK induces centrosome amplification, aneuploidy and transformation. Nat Genet 1998; 20:189–193.
32 McCarthy DM, Hruban RH, Argani P, *et al.* Role of the DPC4 tumor suppressor gene in adenocarcinoma of the ampulla of vater: analysis of 140 cases. Mod Pathol 2003;16:272–278.
33 Bertucci F, Houlgatte R, Benziane A, *et al.* Gene expression profiling of primary breast carcinomas using arrays of candidate genes GATA-3 is expressed in association with estrogen receptor in breast cancer. Hum Mol Genet 2000;9:2981–2991.
34 Hoch RV, Thompson DA, Baker RJ, *et al.* GATA-3 is expressed in association with estrogen receptor in breast cancer. Int J Cancer 1999;84:122–128.
35 Forozan F, Mahlamaki EH, Monni O, *et al.* Comparative genomic hybridization analysis of 38 breast cancer cell lines: a basis for interpreting complementary DNA microarray data. Cancer Res 2000;60:4519–4525.
36 Aubele MM, Cummings MC, Mattis AE, *et al.* Accumulation of chromosomal imbalances from intraductal proliferative lesions to adjacent *in situ* and invasive ductal breast cancer. Diag Mol Patho 2000;9:14–19.
37 Climent J, Martinez-Climent JA, Blesa D, *et al.* Genomic loss of 18p predicts an adverse clinical outcome in patients with high-risk breast cancer. Clin Cancer Res 2002;8:3863–3869.
38 Gaki V, Tsopanomichalou M, Sourvinos G, *et al.* Allelic loss in chromosomal region 1q21-23 in breast cancer is associated with peritumoral angiolymphatic invasion and extensive intraductal component. Eur J Surg Oncol 2000;26:455–460.
39 Bieche I, Champeme MH, Lidereau R. Loss and gain of distinct regions of chromosome 1q in primary breast cancer. Clin Cancer Res 1995;1:123–127.
40 Minobe K, Onda M, Iida A, *et al.* Allelic loss on chromosome 9q is associated with lymph node metastasis of primary breast cancer. Jpn J Cancer Res 1998;89:916–922.
41 Hislop RG, Pratt N, Stocks SC, *et al.* Karyotypic aberrations of chromosomes 16 and 17 are related to survival in patients with breast cancer. Br J Surg 2002;89:1581–1586.
42 Pandis N, Jin Y, Gorunova L, *et al.* Chromosome analysis of 97 primary breast carcinomas: identification of eight karyotypic subgroups. Genes Chromosomes Cancer 1995;12:173–185.

Journal of Mammary Gland Biology and Neoplasia, Vol. 9, No. 3, July 2004 (© 2004)

Centrosome Amplification and the Origin of Chromosomal Instability in Breast Cancer

Jeffrey L. Salisbury,[1,3] Antonino B. D'Assoro,[1] and Wilma L. Lingle[1,2]

The development and progression of aggressive breast cancer is characterized by genomic instability leading to multiple genetic defects, phenotypic diversity, chemoresistance, and poor outcome. Centrosome abnormalities have been implicated in the origin of chromosomal instability through the development of multipolar mitotic spindles. Breast tumor centrosomes display characteristic structural abnormalities, termed *centrosome amplification*, including: increase in centrosome number and volume, accumulation of excess pericentriolar material, supernumerary centrioles, and inappropriate phosphorylation of centrosome proteins. In addition, breast tumor centrosomes also show functional abnormalities characterized by inappropriate centrosome duplication during the cell cycle and nucleation of unusually large microtubule arrays. These observations have important implications for understanding the mechanisms underlying genomic instability and loss of cell polarity in cancer. This review focuses on the coordination of the centrosome, DNA, and cell cycles in normal cells and their deregulation resulting in centrosome amplification and chromosomal instability in the development and progression of breast cancer.

KEY WORDS: aneuploidy; centriole; cell cycle; mitosis.

INTRODUCTION

The centrosome is a fascinating organelle that resides near the cell center (hence its name, see (1)). It functions in the maintenance of cytoplasmic architecture through the nucleation and organization of microtubules in interphase and mitotic cells (2–4). In addition to its fundamental role in microtubule organization, the centrosome may also provide an important structural context for coordinating cell cycle regulation (5,6). Understanding the molecular basis for these diverse cellular functions is beginning to emerge through the careful analysis of centrosome genes and proteins, and centrosome formation, structure, and organization in yeast and in mammalian somatic cells, and in early embryo development in model systems such as *Drosophila* and the nematode (7–9). Recently, a comprehensive catalogue of centrosome composition was determined using mass-spectrometry-based protein correlation profiling in which several proteins linked to the etiology of certain disease processes including cancer were identified as putative centrosome proteins (10).

Centrosome Structure

Structurally, centrosomes consist of four fundamental components: a core structure consisting of a pair of *centrioles* that serve as a centrosomal organizer; a surrounding protein lattice or matrix called *pericentriolar material* (PCM) that serves as a framework to anchor microtubule nucleation sites; *γ-tubulin complexes* that are responsible for the nucleation of microtubules; and finally fibers composed of *Sfi1p* and *centrin* that act as calcium-sensitive

[1] Tumor Biology Program, Mayo Clinic College of Medicine, Mayo Clinic, Rochester, Minnesota.
[2] Division of Experimental Pathology, Mayo Clinic College of Medicine, Mayo Clinic, Rochester, Minnesota.
[3] To whom correspondence should be addressed at Tumor Biology Program, Mayo Clinic College of Medicine, Mayo Clinic, Rochester, Minnesota 55905; e-mail: Salisbury@mayo.edu.

1083-3021/04/0700-0275/0

contractile or elastic connections between the various elements of the centrosome, which mediate dynamic changes in its overall structure and regulate centriole duplication.

Centrioles are small barrel-shaped organelles (~200 nm diameter and 400 nm in length) consisting of a cylindrical array of nine triplet microtubules (11,12). Once during each cell cycle the centrosome duplicates in a process that is initiated with the doubling of centrioles. The centriole pair embodies an intrinsic counting mechanism that establishes the number of functional centrosome equivalents in the cell such that a pair of centrioles equals one, and two pair of centrioles equals two centrosome equivalents (13). Recent studies suggest that centrosome size and organization of PCM depend on the integrity of the centrioles themselves (8,14–16).

Pericentriolar material (PCM) is structurally complex and consists of a lattice or matrix of coiled-coil proteins (7), including pericentrin (17,18), Cep135 (19), AKAP-450 (20,21), and ninein (22). Several of these coiled-coil proteins act as anchors for other essential centrosome proteins and for key regulators of centrosome function. For example, γ-tubulin complexes are anchored to the centrosome by pericentrin (18,23), and protein kinase A is anchored by both pericentrin and the protein kinase A anchoring protein AKAP-450 (21,24). Centrosomes increase in size through the recruitment of PCM, and the two centrosomes of G2/M cells show a dramatic increase in microtubule nucleating activity as they function as spindle poles during mitosis (8).

Centrosome organization is regulated by dynamic behavior of calcium-sensitive fibers, composed of the proteins Sfi1p and centrin that link the centrioles to one another and to the surrounding pericentriolar material, and by their cell cycle-dependent integrity (9,25–27). Remarkably, Sfi1 protein binds multiple centrin molecules along a series of internal repeats, and the complex forms Ca^{2+}-sensitive contractile fibers that function to reorient centrioles and alter centrosome structure.

Centrosome Duplication

The centrosome is duplicated once, and only once, during a normal cell cycle to yield two centrosomes that function as the spindle poles of the dividing cell (28). The process is most clearly illustrated by duplication of the centrioles themselves. In early G1 phase of the cell cycle the two centrioles, which originated in previous cell cycles, are typically oriented in a characteristic arrangement orthogonal to one another. As cells pass the G1 restriction point and commit to DNA replication subsequent to cell division, the two centrioles separate a short distance from one another (centriole disjunction). Nascent *pro*centrioles form at the proximal end orthogonal to each preexisting centriole (29,30). During G2/M phase of the cell cycle, centrosome duplication is completed through a maturation process involving the recruitment of additional PCM protein, and each new centrosome, containing one old and one new centriole, functions as a spindle pole during mitosis. The presence of only two centrosomes in the cell as it enters mitosis ensures the formation of a bipolar spindle and the equal segregation of sister chromatids to each daughter cell. Mitotic spindle poles also play a role in determining the position and orientation of the cleavage furrow and in exit from cytokinesis (31,32). While centriole duplication occurs in a semiconservative fashion in most cells as described above, during development and in certain cells under special experimental circumstances centrioles can arise de novo (33–35).

Coordination of the Centrosome, DNA, and Cell Cycles

Progress in understanding the centrosome duplication cycle has recently accelerated. Centrosome duplication is strictly coordinated with DNA replication, mitosis, and cell division (6). The control of centrosome duplication is tightly coupled to cell cycle progression through pathways of regulation that operate in parallel. The first of these regulatory pathways operates through activity of cell cycle regulators, including Cdk/cyclin A and E, which coordinate the cell, centrosome, and DNA cycles (6,36–38). The second control pathway involves the p53-mediated G1/S and G2/M cell cycle checkpoints that monitor DNA integrity and arrest centrosome duplication through the induction of $p21^{waf1}$ synthesis and consequent inhibition of the cdk/cyclins (39–41). The third regulatory pathway operates through the control of abundance and function of the key centriole proteins and the activation of centrosome-directed kinases and phosphatases.

Evidence suggesting a direct role for the Cdks in regulating the mitotic activity of centrosomes first came to light from studies on the localization of

cyclin B and Cdk1 ($p34^{cdc2}$) at the centrosome during G2/M phase, and from experiments using *Xenopus* cell-free extracts that implicated cyclin A and B in the control of microtubule dynamics (42–45). More recently, the direct involvement of Cdk2 activity in regulation of centrosome duplication was established. Both centrosome duplication and DNA replication are dependent on Cdk2 activation and are blocked by the Cdk2 inhibitors butyrolactone I and roscovitine (38,39,46). Cdk2/cyclin E activity was subsequently identified as a key regulator of the centrosome cycle, since centrosome duplication was blocked by the small protein inhibitors of Cdk2, $p21^{waf1}$ or p27, or by immuno-depletion of Cdk2 or cyclin E, and centrosome duplication was restored by excess purified cdk2/cyclin E (36–39). An early event in the centrosome duplication cycle, the separation of the centriole pair (centriole disjunction), is dependent on Cdk2/cyclin E activity, suggesting that a Cdk-mediated phosphorylation event regulates centriole pair cohesion (37,47).

Additional protein phosphorylation events play key roles in controlling centrosome behavior and function during the cell cycle (48). Centrosome protein phosphorylation increases dramatically at the onset of mitosis and falls precipitously at the metaphase/anaphase transition (49–52). Importantly, several centrosome-associated kinases and target substrates implicated in the regulation of the centrosome cycle become altered during the development of centrosome amplification in cancer (53–56). Finally, centrosome duplication also depends on the phosphorylation status of the retinoblastoma tumor suppressor Rb, which governs the availability of the E2F transcription factor to promote S phase progression (57). Taken together, these findings establish the mechanism by which DNA replication and centrosome duplication are coordinated during the cell cycle: both DNA replication and centrosome duplication are controlled by the Rb pathway and depend on downstream transcriptional consequences of E2F activity, and both processes require Cdk2/cyclin activation.

The Centrosome and DNA Cycles Can Be Uncoupled

In certain cells, multiple rounds of centrosome duplication can occur when DNA replication is blocked, so that the centrosome cycle is not strictly dependent on DNA replication per se (58). However, recent evidence suggests that uncoupling of the centrosome and DNA cycles can occur only in cells that are defective in G1/S checkpoint controls. Several studies suggest that loss of p53 function and certain gain-of-function p53 mutations result in deregulation of centrosome duplication and lead to functionally amplified centrosomes (59–61). The tumor suppressor protein p53 is involved in the control of centrosome duplication through activation of the G1/S checkpoint and transcriptional regulation of several downstream targets including the Cdk inhibitor $p21^{waf1}$ (39–41). $p21^{waf1}$ blocks centrosome duplication through inhibition of Cdk2/cyclin E activity. Moreover, reduced activity of $p21^{waf1}$ by antisense expression in human cell lines resulted in centrosome amplification (62).

Even so, while introduction of wild-type p53 into $p53^{-/-}$ mouse embryonic fibroblasts reestablished centrosome homeostasis, overexpression of $p21^{waf1}$ only partially restored control of centrosome duplication in p53-null fibroblasts (63). Thus other control pathways and downstream targets of p53 may also play important roles in the control of centrosome homeostasis. For example, p53 mutations and cyclin E or cyclin A overexpression act synergistically to further increase the frequency of centrosome amplification in cultured cells and in tumors (39,64).

Recently, we investigated the relationship between G1/S checkpoint integrity and development of centrosome amplification (39). We studied the effect of genotoxic stress in breast tumor derived cell lines with different p53 backgrounds and found that p53 activity, through upregulation of $p21^{WAF1}$ and retinoblastoma hypophosphorylation, is essential for the maintenance of centrosome homeostasis following DNA damage. We also found that loss of p53 function and an abrogated G_1/S cell cycle checkpoint are not sufficient to drive centrosome amplification, but rather the development of centrosome defects required subsequent genotoxic stress to dissociate the DNA and centriole duplication cycles. Taken together, these studies suggest that the p53 pathway and the cdk/cyclins are key players in the regulation of centrosome behavior in normal cells. These findings also suggest that an imbalance between negative and positive cell cycle regulators could accelerate centrosome defects seen in the development of cancer.

It is important to emphasize that during cancer progression, centrosome amplification and genomic instability can also develop independently of loss of p53 function, suggesting the presence of alternative

pathways leading to disregulation of centrosome homeostasis (65–68). Mutations in the BRCA1 and BRCA2 tumor suppressor genes associated with the development of familial breast and ovarian cancers also have been implicated in the loss of control of the centrosome cycle (69). BRCA1 protein localizes at the centrosome during mitosis, and the hypophosphorylated form of BRCA1 coimmunoprecipitates with γ-tubulin (70–72). Mouse embryo fibroblasts carrying gene-targeted deletions in BRCA1 or BRCA2 showed a defective G2/M checkpoint function, amplified centrosomes, aberrant mitoses, and aneuploidy (71,73). GADD45, a downstream transcriptional product of the p53 pathway, has also been implicated in both DNA damage repair and activation of the G2/M checkpoint (74,75). Cells lacking GADD45 expression show centrosome amplification, mitotic spindle defects, and chromosomal instability (76). These studies highlight the evidence that centrosome amplification can develop through alternative pathways that converge on G1/S and/or G2/M checkpoint regulators, implying a link between the control of the centrosome cycle and the DNA repair machinery.

Centrosomes and Cancer

Centrosome defects have been implicated in disease processes, particularly in the origin of mitotic abnormalities and the development of aneuploidy in cancer (77). Recent studies implicate centrosome defects in the origin of chromosomal instability and the pathogenesis of cancer (53,68,78–82). Centrosome defects (i.e., centrosome amplification) are characteristic of many solid tumors. The term "centrosome amplification" signifies centrosomes that contain more than four centrioles (i.e., "supernumerary centrioles"), centrosomes that appear significantly larger than normal as defined by the staining of structural centrosome components in excess of that seen in the corresponding normal tissue or cell type, and/or when more than two centrosomes are present within a cell (53,83,84). In addition, amplified centrosomes also show protein hyperphosphorylation and altered functional properties such as an increased microtubule nucleating capacity (53–55,85,86). These centrosome abnormalities have been implicated in the loss of cell and tissue architecture seen in cancer (i.e., anaplasia) through altered centrosome function in microtubule nucleation and organization, and also in chromosome missegregation during mitosis as a consequence of an increased rate of multipolar spindle formation (Fig. 1) (53,68,87). Together, these observations underscore the importance of proper coordination of the centrosome and cell cycles, and illustrate the potential for severe consequences when proper regulation of these processes fails.

Centrosome Amplification, Chromosomal Instability, and p53 in Human Breast Tumors

Chromosomal abnormalities have long been recognized as a distinguishing feature of cancer cells, and the development of aneusomy may be an early event in breast tumor development (88,89). One mechanism for the origin of genomic instability in cancer is through flux in karyotype or chromosomal instability (CIN), which can give rise to aneuploidy. Operationally, CIN describes the *rate* of change in chromosome number, while aneuploidy is characterized as the *state* of an altered chromosome number (67,90). Because duplicated centrosomes function as the mitotic spindle poles and are responsible for bipolar spindle formation and proper chromosome segregation during mitosis, it has been suggested that centrosome amplification could drive tumor aneuploidy by increasing the frequency of abnormal mitoses that lead to chromosome missegregation (53,54,68,91,92).

In a comprehensive study of normal and malignant human breast tissue, we examined the relationship between centrosome amplification, aneuploidy and CIN, and loss of tissue differentiation (68). Our studies demonstrated for the first time using primary breast tumors that two aspects of centrosome amplification correlate independently with distinct features of breast cancer (53,68,84). Firstly, increased centrosome size and centrosome number correlated with CIN. We further demonstrated that increased centrosome size is present in most in situ lesions, supporting the hypothesis that centrosome abnormalities drive chromosomal aberrations as an early event in DCIS. In addition, increased MT nucleation capacity of centrosomes correlated with loss of tissue differentiation—MT nucleation was significantly greater in tumors with p53 mutations, which also showed significant loss of tissue differentiation as indicated by high histologic grade. Together, these results support the hypothesis that centrosome amplification is an early event in tumorigenesis that drives both chromosomal instability and loss of differentiation through independent centrosome functions.

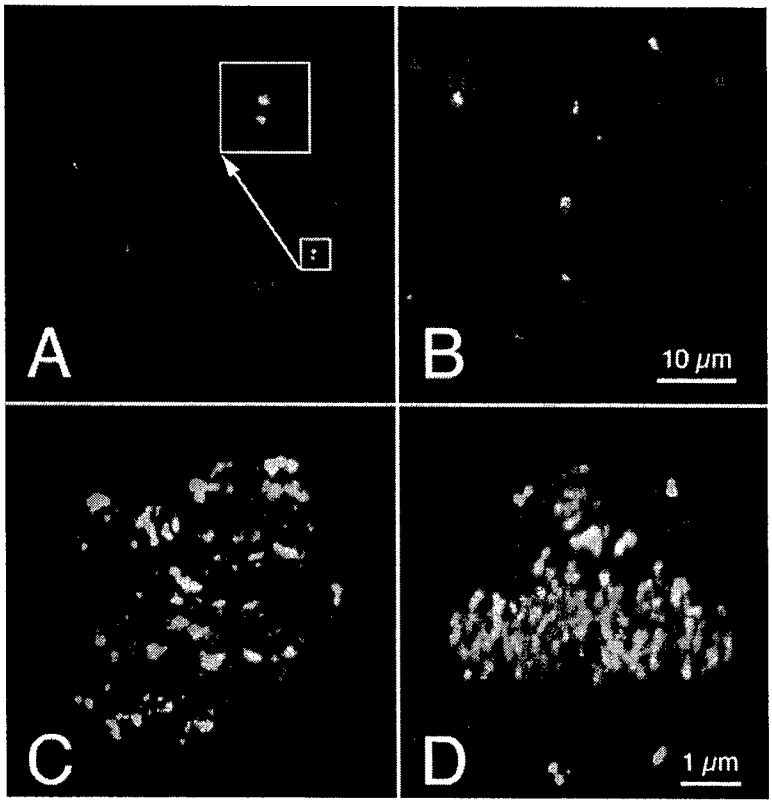

Fig. 1. Breast tumor cell lines with normal (A) or amplified (B) centrosomes. Centrioles are stained green for centrin and pericentriolar material is stained red for pericentrin. Bar = 10 μm. Multipolar spindles (C and D) illustrating the mechanics generating chromosomal instability during mitosis in cells with amplified centrosomes. Centrioles are stained green for centrin, spindle matrix is stained red for the motor protein Eg5, and kinetochores are stained light blue with human autoimmune serum. Bar = 1 μm. DNA is stained blue with Hoechst 33342 in all images.

Interestingly, our studies on human breast tissue also demonstrated that centrosome amplification and aneuploidy occur independently of p53 mutation (68,87). Our results demonstrate that increased MT nucleation capacity is a feature of centrosome amplification that is independent of centrosome number and centrosome size in breast tumors. While MT nucleation capacity did not correlate with CIN or aneuploidy, it was significantly greater in p53 mutant aneuploid tumors than in aneuploid tumors with wild-type p53. MT nucleation capacity did correlate with increased Nottingham Grade, suggesting a relationship between defects in the MT cytoskeleton and loss of tissue differentiation. In single- and multi-center studies, Nottingham Grade predicted clinical outcome, with increasing grade being associated with shorter disease-free survival and overall survival (93–96). Likewise, centrosome amplification correlated with loss of differentiation as defined by increased Gleason score in prostate tumors (92). Together these observations implicate alterations in functional properties of centrosomes in maintaining the morphological changes associated with tumor development.

Although p53 mutation has been suggested as a cause for CIN in breast cancer (97), our results, and results from other studies (68,87,98,99), demonstrate that while aneuploidy and CIN can occur in the absence of p53 mutation, they do not occur in the absence of structural centrosome amplification. While mutant p53 was present in a significant portion of breast tumors, its occurrence was not prerequisite to the development of aneuploidy. In the cases where mutant p53 is a factor, it is likely that

p53 mutation affects centrosome number to promote abnormal mitoses (59,100,101). Our studies further demonstrate that p53 mutations correlate with a significant increase in the MT nucleation capacity of centrosomes.

CONCLUSIONS

Centrosome abnormalities are characteristic of aggressive tumors and arise early in the development of breast cancer. In normal cells, the DNA and centrosome cycles are tightly coupled during the cell cycle through Cdk2/cyclin activation and the Rb pathway, and depend on downstream transcriptional consequences of E2F activity. While loss of p53 function and an abrogated G_1/S cell cycle checkpoint may facilitate the development of centrosome abnormalities in cancer, they are not sufficient to drive centrosome amplification. Rather the development of centrosome defects requires subsequent genotoxic stress to dissociate the DNA and centriole duplication cycles. Centrosome amplification correlates with CIN and possibly drives the development of aneuploidy in human breast tumors through consequent mitotic abnormalities. Thus, in aggressive tumors, centrosome amplification may drive chromosomal instability leading to multiple genetic defects, phenotypic diversity, chemoresistance, and poor outcome. Furthermore, centrosome amplification may increase metastatic potential through cytoskeletal alterations that affect tissue architecture in breast tumors. Centrosome defects may indicate an increased propensity for the development of CIN and unstable karyotypes in breast cancer, and therefore may be useful for the identification of a subset of patients who would benefit from initial aggressive treatment. Finally, the centrosome represents a promising target for therapies against breast cancer through suppression of centrosome duplication and separation, and of the MT nucleation function.

ACKNOWLEDGMENTS

This work was supported by NCI CA72836 to J.L.S, USAMRMC DAMD (BC022276) to A.B.D., USAMRMC DAMD (17-98-1-8122 and 17-01-1-0753) to W.L.L., and the Mayo Clinic Foundation.

REFERENCES

1. Wilson E. B. (1925). *The Cell in Development and Heredity*, 3rd edn. Macmillan, New York.
2. M. Kirschner and T. Mitchison (1986). Beyond self-assembly: From microtubules to morphogenesis. *Cell* **45:**329–342.
3. M. Bornens (2002). Centrosome composition and microtubule anchoring mechanisms. *Curr. Opin. Cell Biol.* **14:**25–34.
4. R. E. Palazzo (2003). Centrosome and spindle pole body dynamics: A review of the EMBO/EMBL Conference on Centrosomes and Spindle Pole Bodies, Heidelberg, September 13–17, *Cell Motil. Cytoskeleton* **54:**148–154.
5. S. J. Doxsey (2001). Centrosomes as command centres for cellular control. *Nat. Cell Biol.* **3:**E105–E108.
6. G. Sluder and E. H. Hinchcliffe (2000). The coordination of centrosome reproduction with nuclear events during the cell cycle. *Curr. Top. Dev. Biol.* **49:**267–289.
7. J. L. Salisbury (2003). Centrosomes: Coiled-coils organize the cell center. *Curr. Biol.* **13:**R88-R90.
8. J. L. Salisbury (2003). Centrosome size is controlled by centriolar SAS-4. Trends *Cell Biol.* **13:**340–343.
9. J. L. Salisbury (2004). Centrosomes: sfi1p and centrin unravel a structural riddle. *Curr. Biol.* **14:**R27-R29.
10. J. S. Andersen, C. J. Wilkinson, T. Mayor, P. Mortensen, E. A. Nigg, and M. Mann (2003). Proteomic characterization of the human centrosome by protein correlation profiling. *Nature* **426:**570–574.
11. S. Dutcher (2001). Motile organelles: The importance of specific tubulin isoforms. *Curr. Biol.* **11:**R419–R22.
12. S. K. Dutcher (2001). The tubulin fraternity: Alpha to eta. *Curr. Opin. Cell Biol.* **13:**49–54.
13. D. Mazia (1987). The chromosome cycle and the centrosome cycle in the mitotic cycle. *Int. Rev. Cytol.* **100:**49–92.
14. Y. Bobinnec, A. Khodjakov, L. M. Mir, C. L. Rieder, B. Edde, and M. Bornens (1998). Centriole disassembly in vivo and its effect on centrosome structure and function in vertebrate cells. *J. Cell Biol.* **143:**1575–1589.
15. M. Kirkham, T. Muller-Reichert, K. Oegema, S. Grill, and A. A. Hyman (2003). SAS-4 is a C. elegans centriolar protein that controls centrosome size. *Cell* **112:**575–587.
16. S. Leidel and P. Gonczy (2003). SAS-4 is essential for centrosome duplication in C. elegans and is recruited to daughter centrioles once per cell cycle. *Dev. Cell* **4:**431–439.
17. S. J. Doxsey, P. Stein, L. Evans, P. D. Calarco, and M. Kirschner (1994). Pericentrin, a highly conserved centrosome protein involved in microtubule organization. *Cell* **76:**639–650.
18. J. B. Dictenberg, W. Zimmerman, C. A. Sparks, A. Young, C. Vidair, Y. Zheng, *et al.* (1998). Pericentrin and gamma-tubulin form a protein complex and are organized into a novel lattice at the centrosome. *J. Cell Biol.* **141:**163–174.
19. T. Ohta, R. Essner, J.-H. Ryu, R. E. Palazzo, Y. Uetake, and R. Kuriyama (2002). Characterization of Cep135, a novel coiled-coil centrosomal protein involved in microtubule organization in mammalian cells. *J. Cell Biol.* **156:**87–100.
20. G. Keryer, R. M. Rios, B. F. Landmark, B. Skalhegg, S. M. Lohmann, and M. Bornens (1993). A high-affinity binding protein for the regulatory subunit of cAMP- dependent

protein kinase II in the centrosome of human cells. *Exp. Cell Res.* **204:**230–240.
21. O. Witczak, B. S. Skalhegg, G. Keryer, M. Bornens, K. Tasken, T. Jahnsen, *et al.* (1999). Cloning and characterization of a cDNA encoding an A-kinase anchoring protein located in the centrosome, AKAP450. *EMBO J.* **18:**1858–1868.
22. V. Bouckson-Castaing, M. Moudjou, D. J. Ferguson, S. Mucklow, Y. Belkaid, G. Milon, *et al.* (1996). Molecular characterisation of ninein, a new coiled-coil protein of the centrosome. *J. Cell Sci.* **109:**179–190.
23. A. Young, J. B. Dictenberg, A. Purohit, R. Tuft, and S. J. Doxsey (2000). Cytoplasmic dynein-mediated assembly of pericentrin and gamma tubulin onto centrosomes. *Mol. Biol. Cell* **11:**2047–2056.
24. D. Diviani, L. K. Langeberg, S. J. Doxsey, and J. D. Scott (2000). Pericentrin anchors protein kinase A at the centrosome through a newly identified RII-binding domain. *Curr. Biol.* **10:**417–420.
25. J. V. Kilmartin (2003). Sfi1p has conserved centrin-binding sites and an essential function in budding yeast spindle pole body duplication. *J. Cell Biol.* **162:**1211–1221.
26. A. T. Baron, V. J. Suman, E. Nemeth, and J. L. Salisbury (1994). The pericentriolar lattice of PtK2 cells exhibits temperature and calcium-modulated behavior. *J. Cell Sci.* **107:**2993–3003.
27. A. T. Baron, T. M. Greenwood, C. W. Bazinet, and J. L. Salisbury (1992). Centrin is a component of the pericentriolar lattice. *Biol. Cell* **76:**383–388.
28. D. R. Kellogg (1989). Centrosomes. Organizing cytoplasmic events. *Nature* **340:**99–100.
29. I. R. Adams and J. V. Kilmartin (2000). Spindle pole body duplication: A model for centrosome duplication? *Trends Cell Biol.* **10:**329–335.
30. D. Wheatley (1982). *The Centriole: A Central Enigma of Cell Biology*, Elsevier Biomedical Press, Amsterdam.
31. A. Khodjakov and C. L. Rieder (2001). Centrosomes enhance the fidelity of cytokinesis in vertebrates and are required for cell cycle progression. *J. Cell Biol.* **153:**237–242.
32. M. Piel, J. Nordberg, U. Euteneuer, and M. Bornens (2001). Centrosome-dependent exit of cytokinesis in animal cells. *Science* **291:**1550–1553.
33. A. Khodjakov, C. L. Rieder, G. Sluder, G. Cassels, O. Sibon, and C.-L. Wang (2002). De novo formation of centrosomes in vertebrate cells arrested during S phase. *J. Cell Biol.* **158:**1171–1181.
34. W. F. Marshall, Y. Vucica, and J. L. Rosenbaum (2001). Kinetics and regulation of de novo centriole assembly. Implications for the mechanism of centriole duplication. *Curr. Biol.* **11:**308–317.
35. W. F. Marshall (1999). No centriole, no centrosome. *Trends Cell Biol.* **9:**94.
36. E. H. Hinchcliffe, C. Li, E. A. Thompson, J. L. Maller, and G. Sluder (1999). Requirement of Cdk2-cyclin E activity for repeated centrosome reproduction in Xenopus egg extracts. *Science* **283:**851–854.
37. K. R. Lacey, P. K. Jackson, and T. Stearns (1999). Cyclin-dependent kinase control of centrosome duplication. *Proc. Natl. Acad. Sci. U.S.A.* **96:**2817–2822.
38. Y. Matsumoto, K. Hayashi, and E. Nishida (1999). Cyclin-dependent kinase 2 (Cdk2) is required for centrosome duplication in mammalian cells. *Curr. Biol.* **9:**429–432.
39. A. D'Assoro, R. Busby, K. Suino, E. Delva, G. Almodovar-Mercado, H. Johnson, *et al.* (in press). Genotoxic stress leads to centrosome amplification in breast cancer cell lines that have an inactive G1/S cell cycle checkpoint. *Oncogene* **23:**4068–4075.
40. W. S. el-Deiry, T. Tokino, V. E. Velculescu, D. B. Levy, R. Parsons, J. M. Trent, *et al.* (1993). WAF1, a potential mediator of p53 tumor suppression. *Cell* **75:**817–825.
41. J. W. Harper, G. R. Adami, N. Wei, K. Keyomarsi, and S. J. Elledge (1993). The p21 Cdk-interacting protein Cip1 is a potent inhibitor of G1 cyclin-dependent kinases. *Cell* **75:**805–816.
42. E. Bailly, J. Pines, T. Hunter, and M. Bornens (1992). Cytoplasmic accumulation of cyclin B1 in human cells: Association with a detergent-resistant compartment and with the centrosome. *J. Cell Sci.* **101:**529–545.
43. A. Debec and C. Montmory (1992). Cyclin B is associated with centrosomes in Drosophila mitotic cells. *Biol. Cell* **75:**121–126.
44. F. Verde, J. C. Labbe, M. Doree, and E. Karsenti (1990). Regulation of microtubule dynamics by cdc2 protein kinase in cell-free extracts of Xenopus eggs. *Nature* **343:**233–238.
45. F. Verde, M. Dogterom, E. Stelzer, E. Karsenti, and S. Leibler (1992). Control of microtubule dynamics and length by cyclin A- and cyclin B-dependent kinases in Xenopus egg extracts. *J. Cell Biol.* **118:**1097–1108.
46. S. M. Keezer and D. M. Gilbert (2002). Sensitivity of the origin decision point to specific inhibitors of cellular signaling and metabolism. *Exp. Cell Res.* **273:**54–64.
47. M. Okuda (2002). The role of nucleophosmin in centrosome duplication. *Oncogene* **21:**6170–6174.
48. A. M. Fry, T. Mayor, and E. A. Nigg (2000). Regulating centrosomes by protein phosphorylation. *Curr. Top. Dev. Biol.* **49:**291–312.
49. D. D. Vandre and G. G. Borisy (1989). Anaphase onset and dephosphorylation of mitotic phosphoproteins occur concomitantly. *J. Cell Sci.* **94:**245–258.
50. D. D. Vandre, Y. Feng, and M. Ding (2000). Cell cycle-dependent phosphorylation of centrosomes: Localization of phosphopeptide specific antibodies to the centrosome. *Microsc. Res. Tech.* **49:**458–466.
51. P. N. Rao, J. Y. Zhao, R. K. Ganju, and C. L. Ashorn (1989). Monoclonal antibody against the centrosome. *J. Cell Sci.* **93:**63–69.
52. W. Lutz, W. L. Lingle, D. McCormick, T. M. Greenwood, and J. L. Salisbury (2001). Phosphorylation of centrin during the cell cycle and its role in centriole separation preceding centrosome duplication. *J. Biol. Chem.* **276:**20774–20780.
53. W. L. Lingle, W. H. Lutz, J. N. Ingle, N. J. Maihle, and J. L. Salisbury (1998). Centrosome hypertrophy in human breast tumors: Implications for genomic stability and cell polarity. *Proc. Natl. Acad. Sci. U.S.A.* **95:**2950–2955.
54. H. Zhou, J. Kuang, L. Zhong, W. L. Kuo, J. W. Gray, A. Sahin, *et al.* (1998). Tumour amplified kinase STK15/BTAK induces centrosome amplification, aneuploidy and transformation. *Nat. Genet.* **20:**189–193.
55. Y. Miyoshi, K. Iwao, C. Egawa, and S. Noguchi (2001). Association of centrosomal kinase STK15/BTAK mRNA expression with chromosomal instability in human breast cancers. *Int. J. Cancer* **92:**370–373.

56. H. Katayama, H. Zhou, Q. Li, M. Tatsuka, and S. Sen (2001). Interaction and feedback regulation between STK15/BTAK/Aurora-A kinase and Protein Phosphatase 1 through mitotic cell division cycle. *J. Biol. Chem.* **276:**46219–46224.
57. P. Meraldi, J. Lukas, A. Fry, J. Bartek, and E. Nigg (1999). Centrosome duplication in mammalian somatic cells requires E2F and Cdk2-cyclin A. *Nat. Cell Biol.* **1:**88–93.
58. R. Balczon, L. Bao, W. E. Zimmer, K. Brown, R. P. Zinkowski, and B. R. Brinkley (1995). Dissociation of centrosome replication events from cycles of DNA synthesis and mitotic division in hydroxyurea-arrested Chinese hamster ovary cells. *J. Cell Biol.* **130:**105–115.
59. K. Fukasawa, T. Choi, R. Kuriyama, S. Rulong, and G. F. Vande Woude (1996). Abnormal centrosome amplification in the absence of p53. *Science* **271:**1744–1747.
60. K. L. Murphy and J. M. Rosen (2000). Mutant p53 and genomic instability in a transgenic mouse model of breast cancer. *Oncogene* **19:**1045–1051.
61. P. Tarapore, Y. Tokuyama, H. F. Horn, and K. Fukasawa (2001). Difference in the centrosome duplication regulatory activity among p53 "hot spot" mutants: Potential role of Ser 315 phosphorylation-dependent centrosome binding of p53. *Oncogene* **20:**6851–6863.
62. C. Mantel, S. E. Braun, S. Reid, O. Henegariu, L. Liu, G. Hangoc, *et al.* (1999). p21(cip-1/waf-1) deficiency causes deformed nuclear architecture, centriole overduplication, polyploidy, and relaxed microtubule damage checkpoints in human hematopoietic cells. *Blood* **93:**1390–1398.
63. P. Tarapore, H. F. Horn, Y. Tokuyama, and K. Fukasawa (2001). Direct regulation of the centrosome duplication cycle by the p53- p21Waf1/Cip1 pathway. *Oncogene* **20:**3173–3184.
64. J. G. Mussman, H. F. Horn, P. E. Carroll, M. Okuda, P. Tarapore, L. A. Donehower, *et al.* (2000). Synergistic induction of centrosome hyperamplification by loss of p53 and cyclin E overexpression. *Oncogene* **19:**1635–1646.
65. L. A. Donehower, M. Harvey, B. L. Slagle, M. J. McArthur, C. A. Montgomery, Jr., J. S. Butel, *et al.* (1992). Mice deficient for p53 are developmentally normal but susceptible to spontaneous tumours. *Nature* **356:**215–221.
66. J. R. Eshleman, G. Casey, M. E. Kochera, W. D. Sedwick, S. E. Swinler, M. L. Veigl, *et al.* (1998). Chromosome number and structure both are markedly stable in RER colorectal cancers and are not destabilized by mutation of p53. *Oncogene* **17:**719–725.
67. C. Lengauer, K. Kinzler, and B. Vogelstein (1997). Genetic instability in colorectal cancers. *Nature* **386:**623–627.
68. W. L. Lingle, S. L. Barrett, V. C. Negron, A. B. D'Assoro, K. Boeneman, W. Liu, *et al.* (2002). Centrosome amplification drives chromosomal instability in breast tumor development. *Proc. Natl. Acad. Sci. U.S.A.* **99:**1978–1983.
69. C. X. Deng and S. G. Brodie (2000). Roles of BRCA1 and its interacting proteins. *Bioessays* **22:**728–737.
70. L. C. Hsu and R. L. White (1998). BRCA1 is associated with the centrosome during mitosis. *Proc. Natl. Acad. Sci. U.S.A.* **95:**12983–12988.
71. X. Xu, Z. Weaver, S. P. Linke, C. Li, J. Gotay, X. W. Wang, *et al.* (1999). Centrosome amplification and a defective G2-M cell cycle checkpoint induce genetic instability in BRCA1 exon 11 isoform-deficient cells. *Mol. Cell* **3:**389–395.
72. G. G. Maul, D. E. Jensen, A. M. Ishov, M. Herlyn, and F. J. Rauscher 3rd. (1998). Nuclear redistribution of BRCA1 during viral infection. *Cell Growth Differ.* **9:**743–755.
73. A. Tutt, A. Gabriel, D. Bertwistle, F. Connor, H. Paterson, J. Peacock, *et al.* (1999). Absence of Brca2 causes genome instability by chromosome breakage and loss associated with centrosome amplification. *Curr. Biol.* **9:**1107–1110.
74. M. B. Kastan, Q. Zhan, W. S. el-Deiry, F. Carrier, T. Jacks, W. V. Walsh, *et al.* (1992). A mammalian cell cycle checkpoint pathway utilizing p53 and GADD45 is defective in ataxia-telangiectasia. *Cell* **71:**587–597.
75. X. W. Wang, Q. Zhan, J. D. Coursen, M. A. Khan, H. U. Kontny, L. Yu, *et al.* (1999). GADD45 induction of a G2/M cell cycle checkpoint. *Proc. Natl. Acad. Sci. U.S.A.* **96:**3706–3711.
76. M. C. Hollander, M. S. Sheikh, D. V. Bulavin, K. Lundgren, L. Augeri-Henmueller, R. Shehee, *et al.* (1999). Genomic instability in Gadd45a-deficient mice. *Nat. Genet.* **23:**176–184.
77. B. R. Brinkley (2001). Managing the centrosome numbers game: From chaos to stability in cancer cell division. *Trends Cell Biol.* **11:**18–21.
78. L. M. Gustafson, L. L. Gleich, K. Fukasawa, J. Chadwell, M. A. Miller, P. J. Stambrook, *et al.* (2000). Centrosome hyperamplification in head and neck squamous cell carcinoma: A potential phenotypic marker of tumor aggressiveness. *Laryngoscope* **110:**1798–1801.
79. K. K. Kuo, N. Sato, K. Mizumoto, N. Maehara, H. Yonemasu, C. G. Ker, *et al.* (2000). Centrosome abnormalities in human carcinomas of the gallbladder and intrahepatic and extrahepatic bile ducts. *Hepatology* **31:**59–64.
80. G. A. Pihan, A. Purohit, J. Wallace, H. Knecht, B. Woda, P. Quesenberry, *et al.* (1998). Centrosome defects and genetic instability in malignant tumors. *Cancer Res.* **58:**3974–3985.
81. N. Sato, K. Mizumoto, M. Nakamura, K. Nakamura, M. Kusumoto, H. Niiyama, *et al.* (1999). Centrosome abnormalities in pancreatic ductal carcinoma. *Clin. Cancer Res.* **5:**963–970.
82. R. G. Weber, J. M. Bridger, A. Benner, D. Weisenberger, V. Ehemann, G. Reifenberger, *et al.* (1998). Centrosome amplification as a possible mechanism for numerical chromosome aberrations in cerebral primitive neuroectodermal tumors with TP53 mutations. *Cytogenet Cell Genet* **83:**266–269.
83. A. B. D'Assoro, W. L. Lingle, and J. L. Salisbury (2002). Centrosome amplification and the development of cancer. *Oncogene* **21:**6146–6153.
84. W. L. Lingle and J. L. Salisbury (1999). Altered centrosome structure is associated with abnormal mitoses in human breast tumors. *Am. J. Pathol.* **155:**1941–1951.
85. P. Meraldi, R. Honda, and E. A. Nigg (2002). Aurora-A overexpression reveals tetraploidization as a major route to centrosome amplification in p53−/− cells. *EMBO J.* **21:**483–492.
86. J. L. Salisbury, W. L. Lingle, R. A. White, L. E. Cordes, and S. Barrett (1999). Microtubule nucleating capacity of centrosomes in tissue sections. *J. Histochem. Cytochem.* **47:**1265–1274.
87. A. B. D'Assoro, S. L. Barrett, C. Folk, V. C. Negron, K. Boeneman, and R. C. Busby, *et al.* (2002). Amplified centrosomes in breast cancer: A potential indicator of tumor aggressiveness. *Breast Cancer Res. Treat.* **75:**25–34.
88. J. Mendelin, M. Grayson, T. Wallis, and D. W. Visscher (1999). Analysis of chromosome aneuploidy in breast

carcinoma progression by using fluorescence in situ hybridization. *Lab. Invest.* **79:**387–393.
89. M. Tirkkonen, M. Tanner, R. Karhu, A. Kallioniemi, J. Isola, and O. P. Kallioniemi (1998). Molecular cytogenetics of primary breast cancer by CGH. *Genes Chromosomes Cancer* **21:**177–184.
90. C. Lengauer, K. W. Kinzler, and B. Vogelstein (1998). Genetic instabilities in human cancers. *Nature* **396:**643–649.
91. T. Boveri (1914). *Zur Frage der Entstehung maligner Tumoren*, Fischer Verlag, Jena, Germany (1929 English translation by M. Boveri reprinted as The Origin of Malignant Tumors, The Williams and Wilkins Co., Baltimore).
92. G. A. Pihan, A. Purohit, J. Wallace, R. Malhotra, L. Liotta, and S. J. Doxsey (2001). Centrosome defects can account for cellular and genetic changes that characterize prostate cancer progression. *Cancer Res.* **61:**2212–2219.
93. C. W. Elston and I. O. Ellis (1991). Pathological prognostic factors in breast cancer. I. The value of histological grade in breast cancer: Experience from a large study with long-term follow-up. *Histopathology* **19:**403–410.
94. R. Engers and H. E. Gabbert (2000). Mechanisms of tumor metastasis: Cell biological aspects and clinical implications. *J. Cancer Res. Clin. Oncol.* **126:**682–692.
95. P. L. Fitzgibbons, D. L. Page, D. Weaver, A. D. Thor, D. C. Allred, G. M. Clark, *et al.* (2000). Prognostic factors in breast cancer. College of American Pathologists Consensus Statement *Arch. Pathol. Lab. Med.* **124:**966–978.
96. D. L. Page, R. Gray, D. C. Allred, L. G. Dressler, A. K. Hatfield, S. Martino, *et al.* (2001). Prediction of node-negative breast cancer outcome by histologic grading and S-phase analysis by flow cytometry: An Eastern Cooperative Oncology Group Study (2192). *Am. J. Clin. Oncol.* **24:**10–18.
97. S. Sigurdsson, S. K. Bodvarsdottir, K. Anamthawat-Jonsson, M. Steinarsdottir, J. G. Jonasson, H. M. Ogmundsdottir, *et al.* (2000). p53 abnormality and chromosomal instability in the same breast tumor cells. *Cancer Genet. Cytogenet.* **121:**150–155.
98. C. Lavarino, V. Corletto, A. Mezzelani, G. Della Torre, C. Bartoli, C. Riva, *et al.* (1998). Detection of TP53 mutation, loss of heterozygosity and DNA content in fine-needle aspirates of breast carcinoma. *Br. J. Cancer* **77:**125–130.
99. T. Sauer, K. Beraki, P. W. Jebsen, E. Ormerod, and O. Naess (1998). Numerical aberrations of chromosome 17 in interphase cell nuclei of breast carcinoma cells: Lack of correlation with abnormal expression of p53, neu and nm23 protein. *APMIS* **106:**921–927.
100. S. Chiba, M. Okuda, J. G. Mussman, and K. Fukasawa (2000). Genomic convergence and suppression of centrosome hyperamplification in primary p53−/− cells in prolonged culture. *Exp. Cell Res.* **258:**310–321.
101. P. E. Carroll, M. Okuda, H. F. Horn, P. Biddinger, P. J. Stambrook, L. L. Gleich, *et al.* (1999). Centrosome hyperamplification in human cancer: Chromosome instability induced by p53 mutation and/or Mdm2 overexpression. *Oncogene* **18:**1935–1944.

Estrogen mediates Aurora-A overexpression, centrosome amplification, chromosomal instability, and breast cancer in female ACI rats

Jonathan J. Li*†, S. John Weroha*, Wilma L. Lingle‡, Dan Papa*, Jeffrey L. Salisbury‡, and Sara Antonia Li*

*Hormonal Carcinogenesis Laboratory, Department of Pharmacology, Toxicology, and Experimental Therapeutics, University of Kansas Medical Center, Kansas City, KS 66160; and ‡The Tumor Biology Program, Division of Experimental Pathology, Mayo Clinic and Foundation, Rochester, MN 55905

Communicated by Elwood V. Jensen, University of Cincinnati College of Medicine, Cincinnati, OH, November 8, 2004 (received for review January 16, 2004)

Estrogens play a crucial role in the causation and development of sporadic human breast cancer (BC). Chromosomal instability (CIN) is a defining trait of early human ductal carcinoma *in situ* (DCIS) and is believed to precipitate breast oncogenesis. We reported earlier that 100% of female ACI (August/Copenhagen/Irish) rats treated with essentially physiological serum levels of 17β-estradiol lead to mammary gland tumors with histopathologic, cellular, molecular, and ploidy changes remarkably similar to those seen in human DCIS and invasive sporadic ductal BC. Aurora-A (Aur-A), a centrosome kinase, and centrosome amplification have been implicated in the origin of aneuploidy via CIN. After 4 mo of estradiol treatment, levels of Aur-A and centrosomal proteins, γ-tubulin and centrin, rose significantly in female ACI rat mammary glands and remained elevated in mammary tumors at 5–6 mo of estrogen treatment. Centrosome amplification was initially detected at 3 mo of treatment in focal dysplasias, before DCIS. At 5–6 mo, 90% of the mammary tumor centrosomes were amplified. Comparative genomic hybridization revealed nonrandom amplified chromosome regions in seven chromosomes with a frequency of 55–82% in 11 primary tumors each from individual rats. Thus, we report that estrogen is causally linked via estrogen receptor α to Aur-A overexpression, centrosome amplification, CIN, and aneuploidy leading to BC in susceptible mammary gland cells.

More than 90% of all human breast cancer (BC) cases are sporadic (1). Numerous epidemiological and animal studies show that both endogenous and exogenously ingested estrogens (Es) play a central, if not paramount, role in the causation and development of human sporadic BC (2–6). Recent epidemiological studies show only a minimal rise in BC risk in postmenopausal women taking E replacement therapy over varying periods of use (7–9). In premenopausal women, however, all of the well established risk factors clearly implicate Es in the causation of BC (2–6). In this latter group, 17β-estradiol (E_2) concentrations, all in the low picogram range, within narrow limits of serum and breast tissue levels (10–13), are sufficient to increase sporadic BC risk. Therefore, it is essential to gain a better understanding of how Es, at these physiological concentrations, elicit their oncogenic effects in susceptible target tissues.

Chromosomal instability (CIN) and aneuploidy are defining traits of early human BC ductal carcinoma *in situ* (DCIS) and primary invasive ductal BCs. These distinguishing characteristics of human BC have been seen in 55–78% of the DCISs and in 85–92% of invasive ductal BCs (14–17). Aneuploidy has been a reliable biomarker for BC for many decades. However, it has not been realized until now that it provides an important clue to the causation of sporadic human BC and the involvement of Es in its etiology.

Overexpression of a centrosome kinase, Aurora-A (Aur-A), centrosome amplification, and CIN invariably occur together (18, 19). Centrosome amplification, found in human BC, may play a key role in the origin of CIN and aneuploidy (20–22). Errors in centrosome duplication/separation, frequently found (>90%) in DCIS and in primary invasive ductal BC, are characterized by the development of supernummery centrosomes resulting in the assembly of multipolar spindles during mitosis (21–23). As a result, the maintenance of the diploid genome is lost through CIN leading to the development of tumor cell heterogeneity in BC. Moreover, it has been suggested that Aur-A may have a role in controlling chromosomal segregation events because it specifically associates with interphase centrosomes, mitotic spindle poles and microtubules, and the spindle midbody (24, 25). Overexpression of Aur-A has been shown to effect neoplastic transformation of mammalian cells, both *in vivo* and *in vitro* (25, 26), and occurs with high frequency (>90%) in human DCISs and in primary invasive ductal BCs (27, 28). The studies presented herein link E exposure to the overexpression of Aur-A, γ-tubulin, and centrin, as well as to centrosome amplification, CIN, and aneuploidy, and ultimately to mammary gland tumor (MGT) development. Importantly, these events occur at or nearly physiological, albeit constant, serum E_2 concentrations in susceptible murine breast cells.

Materials and Methods

Animals and Treatment. Intact, cycling female ACI (August/Copenhagen/Irish) rats, 6 weeks old and weighing 90–110 g (Harlan–Sprague–Dawley, Indianapolis), were housed in facilities certified by the AAALAC. The rats were acclimated for 1 week before treatment. They were maintained on a 12-h light/dark cycle, fed ad libitum Teklad Rodent Diet 8604 and tap water, and divided into three groups of 20 rats each. Group 1 received either no treatment or a 20-mg pellet of cholesterol. Groups 2 and 3 received either a single E_2 pellet containing 2 or 3 mg of E_2 plus 18 or 17 mg of cholesterol, respectively. The pellets (Hormone Pellet Press, Shawnee Mission, KS) were implanted in the shoulder region as reported in refs. 5 and 14. The rats were killed at 3, 4, 5, and 6 mo of treatment. Over this period, the serum E_2 concentrations ranged from 55 to 85 pg/ml and from 110 to 140 pg/ml after a 2- or 3-mg dose of E_2, respectively, as reported in ref. 5. At either E_2 dose, 100% MGT incidences were obtained, albeit the MGTs were modestly larger and more numerous at the higher dose. Rats were killed by decapitation and immediately subjected to macroscopic examination for the presence of MGTs, and the number and site were recorded. The abdominal inguinal mammary glands (MGs) were quickly removed. Portions of the MGs and MGTs were immediately frozen in liquid nitrogen and stored at −80°C, whereas others were fixed in 10% buffered formalin, embedded in paraffin, sectioned at 5–6 μm, and stained with hematoxylin/eosin. The spleens of the untreated rats were rapidly placed in 5 ml of RPMI medium 1640 (BioWhittaker) with L-glutamine for immediate processing and cell culture.

Abbreviations: Aur-A, Aurora-A; BC, breast cancer; CGH, comparative genomic hybridization; CIN, chromosomal instability; DCIS, ductal carcinoma *in situ*; E, estrogen; E_2, 17β-estradiol; MG, mammary gland; MGT, MG tumor.

†To whom correspondence should be addressed at: Department of Pharmacology, Mail Stop 1018, University of Kansas Medical Center, 3901 Rainbow Boulevard, Kansas City, KS 66160. E-mail: jli1@kumc.edu.

Immunoprecipitation and Western Blot Analysis. All immunoblots were performed according to standard procedures by using individual MG and tumor cytosolic fractions from six to eight female ACI rats per group. The tissue samples were homogenized with a polytron in a lysate buffer containing 50 mM Tris·HCl (pH 7.4), 0.2 M NaCl, 2 mM EDTA, and a mixture of protease and phosphatase inhibitors, as reported in ref. 5. The total protein concentration was determined with bicinchoninic acid reagents (Pierce), and equal amounts of protein (100 μg) were resolved by SDS/PAGE and electrotransferred to nitrocellulose membranes. Membranes were probed with a γ-tubulin rabbit polyclonal antibody (H-183, Santa Cruz Biotechnology). Proteins were detected by using chemiluminescence (Amersham Pharmacia). Equal loading was confirmed by Coomassie blue staining and immunolabeling of β-actin (I-19, Santa Cruz Biotechnology) of the same membranes. For Aur-A immunoprecipitation, equal amounts of protein (1,000 μg) were precleared with the appropriate IgG corresponding to the host species of the primary antibody, together with agarose conjugate, and incubated at 4°C for 30 min. Following the standard Santa Cruz Biotechnology protocol, immune complexes were discarded, and the supernatant was incubated by mixing at 4°C overnight with 2 μg of Aur-A-1 antibody (L-18, Santa Cruz Biotechnology) and A/G-agarose beads. Proteins were transferred onto nitrocellulose membranes. For centrin immunoprecipitation, protein aliquots (1,000 μg) were incubated with 2 μg of MC1 anti-centrin (prepared in the laboratory of J.L.S.) and precipitated with A/G agarose as described above. After SDS/PAGE, the gels were treated as described by Errabolu *et al.* (29). The blots were visualized by chemiluminescence. Densitometry of Western blots and immunoprecipitation analyses were quantitated by using a Molecular Dynamics Personal Densitometer and IMAGEQUANT software.

RT-PCR. Tissue total RNA was extracted by polytron homogenization, using 1 ml of TRIzol per 100 mg of tissue. After centrifugation, each sample was treated with 0.2 vol of chloroform, shaken, and centrifuged. The total RNA was precipitated with isopropanol and dissolved in diethyl pyrocarbonate-water. RNA concentration was determined by 260-nm absorbance. The exponential range of amplification was determined by varying the number of PCR cycles for each cDNA and a set of two primers, forward 5′-GGCGAATGCTTT GTCCTACT and reverse 5′-CCGTCACAAAGTCAGGGAAT. These primers represent a specific sequence of the catalytic domain of Aur-A. RT-PCR was conducted by using the Invitrogen standard protocol for Moloney murine leukemia virus reverse transcriptase and *Taq* recombinant DNA polymerase, according to the manufacturer's instructions. PCR products were separated on 1.5% agarose gels and visualized with ethidium bromide. The PCR product size was 350 bases. For actin, the forward primer was GGCATCCTGACCCTGAAGTA, the reverse primer was GCCATCTCTTGCTCGAAGTC, and the PCR product was 497 bases.

Centrosome Amplification: Number and Volume. Centrosome amplification was assessed by confocal microscopy of paraffin sections immunolabeled with a monoclonal antibody against the centrosomal protein γ-tubulin (Sigma clone gtu-88C) (30, 31). Determinations made were based on average values of centrosomes in four randomly selected fields of view. A minimum of 100 centrosomes were analyzed from untreated ACI rat MG epithelial tissue, ductal cells with and without dysplasia, cells confined to DCIS, and primary E_2-induced tumors, derived from three to five individual rats. Although fields of E_2-induced primary MGT cells largely exhibited uniform centrosome amplification, robust centrosome amplification in fields of lobular–alveolar hyperplasia was only seen when it coincided with groups of focal dysplastic cells. Centrosomes were scored as amplified if they were larger in size and/or number than seen in normal, untreated rat mammary epithelial tissue. Centrosome area (size) was measured in maximum intensity projections of seven consecutive 0.5-μm optical sections. Centrosomes were scored as amplified in size when their measured area was more than two times the average seen in untreated MGs. A cutoff of 2 times larger was established to exclude centrosomes equivalent in size to late G_2 centrosomes of normal tissues. Additionally, centrosomes were scored as amplified in number when a cluster of more than two centrosomes was associated with a single nucleus.

Spleen Culture and Chromosome Preparation. Spleens from untreated, female ACI rats were cultured as reported in ref. 14. Cell culture suspensions (25 ml) were incubated at 37°C for 4–5 days, with 150 μl of Con A and 30 μl of 0.5% 2-mercaptoethanol. Before harvesting, the spleen cell suspensions were treated with colcemid.

DNA Isolation and Labeling for Comparative Genomic Hybridization (CGH) Analysis. Individual untreated MGs and MGTs were quickly frozen in liquid N, and the DNA was extracted by the LiCl protocol (32). A nick translation kit (Vysis) was used for direct DNA labeling for CGH, according to the manufacturer's recommendations. The probe preparation, hybridization, and posthybridization steps were carried out according to the University of Colorado Health Science Center, Cancer Center Cytogenetics Core FISH Protocol 12 "CGH with Directly Labeled Probes." CGH analyses were performed in an average of 10 metaphase spreads per individual MGT as we have reported (33). Chromosomes were identified by using digitally inverted images of DAPI-banded metaphases and an ACI rat idiogram implemented in the image analysis software. For CGH detection of regional gains and losses, thresholds of 1.20 and 0.80 for over- and underrepresentation were used, respectively. Ratio profiles were generated with the CGH package of QUIPS software (Vysis) and displayed along with idiograms of rat chromosomes. Fluorescence ratio values exceeding the thresholds were regarded as copy gains (fluorescence ratio >1.2) or losses (fluorescence ratio <0.8). As a precaution against region- or band-specific ratio

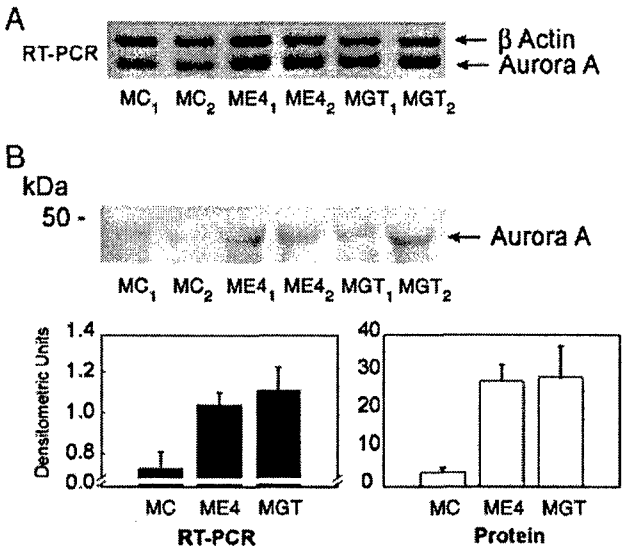

Fig. 1. Expression of Aur-A gene (*A*) and protein (*B*) in untreated MGs, E_2-treated MGs, and E_2-induced MGTs. Representative individual samples of age-matched, untreated control (MC_{1-2}), 4.0-mo ($ME4_{1-2}$), and E_2-induced MGTs (MGT_{1-2}) were used. (*A*) Electrophoretic image of RT-PCR of Aur-A and β-actin mRNA, used as an internal control. RNA processing, primer details, and RT-PCR conditions are described in *Materials and Methods*. *B Upper* shows a Western blot of the relative expression of immunoprecipitated Aur-A in the same treatment groups. *B Lower* shows the Aur-A mRNA (■) and protein (□) relative expression. The values represent the mean ± SE (n = 8).

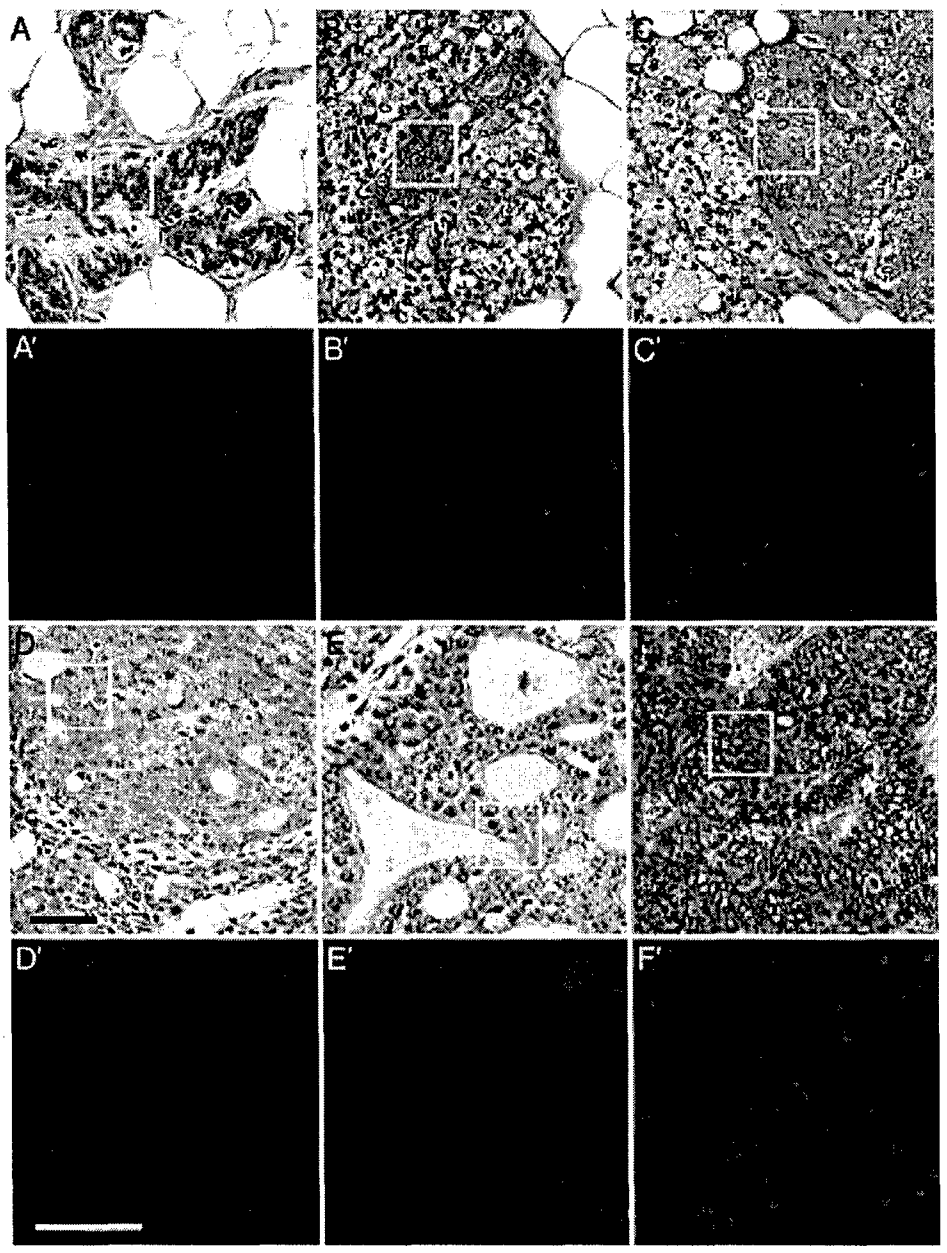

Fig. 2. Centrosome amplification. Centrosomes and nuclei were observed by confocal microscopy of sections labeled with an antibody against γ-tubulin (red) and DNA dye Hoechst 33342 (blue) (*A'–F'*) in areas corresponding to hematoxylin/eosin-stained sections (*A–F*). (*A* and *A'*) Untreated rats. Centrosomes in ductal cells are apical to the nucleus and often appear as a pair of adjacent spots. The size of the centrosome spots, including those in the fibroblast at the bottom of *A'*, is uniform. (*B* and *B'*) dysplasia after 3.0 mo of E_2 treatment. Centrosomes are often larger than those from untreated rats. (*C* and *C'*) Dysplasia after 4 mo of treatment. Centrosomes are often amplified in number and size. (*D* and *D'*) DCIS after 5 mo of treatment. Centrosome amplification in size and number is evident. (*E* and *E'*) DCIS after 6 mo of treatment. Many centrosomes are much larger and often more numerous than centrosomes in control tissues. (*F* and *F'*) E_2-induced MGT. Centrosomes are consistently amplified in both size and number. (Black scale bar, 45 μm; white scale bar, 20 μm.)

fluctuations, CGH hybridizations were verified by exchanging fluorescent labels in the tumor and reference DNA, as described in refs. 34 and 35. For CGH analyses, a criterion of ≥30% frequency of occurrence within any given tumor was considered as a nonrandom/consistent amplified/deleted region.

Statistical Analysis. The significance of differences in protein/RNA expression and centrosome amplification between experimental groups was determined by using Student's *t* test. The data for the CGH analysis were analyzed by the exact binomial distribution test that determines the occurrence/nonoccurrence of an event.

Results

Aur-A Kinase mRNA and Protein Expression. Aur-A mRNA (Fig. 1*A*) and protein (Fig. 1*B*) expression were assessed in control MGs and primary MGTs from 4-mo E_2-treated ACI rats. Employing RT-PCR, a 1.4- and a 1.5-fold increase in Aur-A mRNA was detected after 4 mo of E_2 treatment and in primary MGTs, respectively, compared with age-matched untreated MGs (Fig. 1*A*). Western blot analyses showed a 7.2-fold increase in Aur-A protein expression after 4 mo of E_2 treatment, compared with age-matched control MGs, whereas primary MGTs exhibited a 7.4-fold rise (Fig. 1*B*).

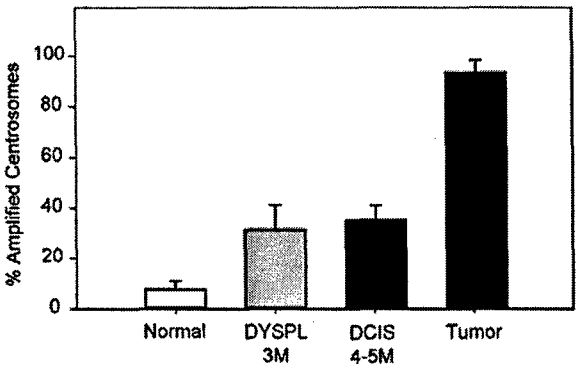

Fig. 3. The percentage of amplified centrosomes relative to untreated MG controls in ductal cells without atypia after 3 mo of E_2 treatment is 7% compared with 30% in dysplastic cells (DYSPL) after 3 mo of treatment. Amplification increased from 30% to 38% in DCIS after 4 and 5 mo of E_2 treatment, respectively, while 90% of MGT centrosomes were amplified.

Centrosome Amplification. Untreated cycling female ACI rat MG epithelial tissue exhibited normal position and complement of centrosomal protein γ-tubulin by immunofluorescence staining. The γ-tubulin labeling was confined to the pair of centrioles apical to the nucleus and proximate to the luminal membrane (Fig. 2*A*). All untreated ACI rat MG tissues showed comparable levels of γ-tubulin immunostaining, including epithelial, myoepithelial, and stromal cells. Similarly, unaffected MG tissue adjacent to E_2-induced MGTs also exhibited normal centrosome staining distribution. However, E_2-induced MGTs showed a markedly elevated number of centrosomes, which were larger and lacking the organized distribution seen in untreated control MG cells (Fig. 2 *F* and *F'*). Centrosome amplification was evident in dysplasia as early as 3 mo after E_2 treatment (Fig. 2 *B*, *B'*, *C*, and *C'*). After 4 and 5 mo of E_2 treatment, a significant increase ($P < 0.002$) in centrosome amplification was detected in groups of cells residing in DCISs (Fig. 2 *D*, *D'*, *E*, and *E'*). However, other cells within the same DCISs exhibited a normal complement of centrosomes. The DCISs after 4 and 5 mo of E_2 treatment were predominantly cribriform (ER^+/PR^+), whereas papillary, comedo, and solid types were less common. With respect to the γ-tubulin staining marker (Fig. 3), 30% of centrosomes were amplified in areas of dysplasias at 3 mo ($P < 0.002$), whereas 38% were amplified in DCIS after 4 mo ($P < 0.002$). In primary MGTs, ≈90% of the centrosomes observed were amplified ($P < 0.001$). Conversely, in ducts without atypia, only 7% of the centrosomes were amplified after 3 mo of E_2 treatment. These results indicate that centrosome amplification is an early event that becomes more pronounced during progression to frank MGTs.

Centrosome Protein Expression. A single γ-tubulin band was evident in untreated MGs (Fig. 4*A*). Two forms of γ-tubulin (γ_f: fast, 50 kDa; and γ_s: slow, 52 kDa) were observed in MGTs. After 4 mo of E_2-treatment, the γ_f-tubulin was reduced and the γ_s-tubulin was increased (Fig. 4*A*). In E_2-induced MGTs, a 2.4-fold rise was observed in total ($\gamma_f + \gamma_s$) γ-tubulin when compared with untreated MGs, whereas a rise of 1.4-fold was detected after 4 mo of E_2 treatment. Centrin levels were increased 11.2-fold in the MGTs compared with untreated MGs (Fig. 4*B*). These results are consistent with the centrosome amplification detected in both E_2-induced DCISs and primary MGTs reported here.

CIN: CGH Analysis. CGH analyses, employing MGT DNA from female ACI rats, showed consistent regional genomic alterations in 11 E_2-induced MGTs derived from individual rats. Analysis of 10–12 CGH metaphase spreads from each E_2-induced primary

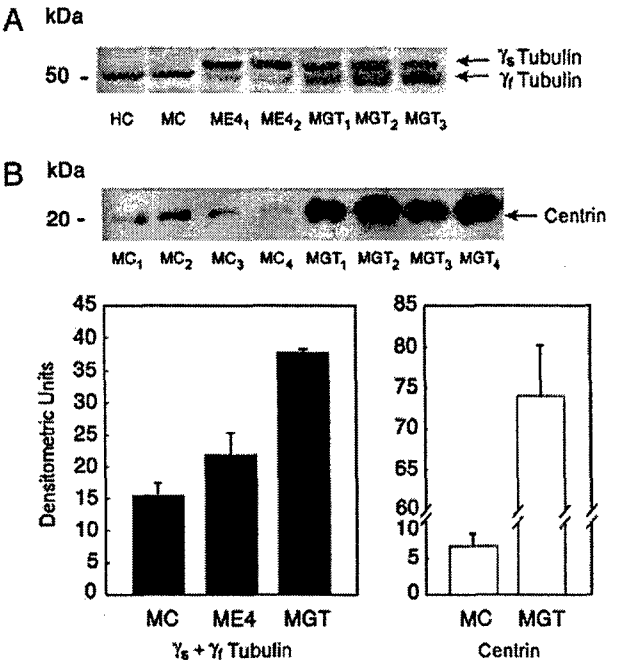

Fig. 4. Immunoblot analysis of the relative expression of γ-tubulin (*A*) and centrin (*B*) in untreated MGs, E_2-treated MGs, and E_2-induced MGTs. Whole-cell lysates from HeLa cells (HC), used as a positive control; age-matched untreated control, MC; 4-mo treated, $ME4_{1-2}$; and E_2-induced MGT_{1-2} were prepared. (*A*) For γ-tubulin, 100-μg protein fractions were examined by Western analysis. (*B*) For centrin, 1,000-μg protein fractions were immunoprecipitated as described in *Material and Methods*. *Lower* shows the relative expression of γ_s-tubulin + γ_f-tubulin (■) and centrin (□). The values represent the mean ± SE ($n = 6$).

MGT revealed nonrandom amplified regions in chromosomes 1, 4, 7, 9, 11, 13, and 20. The consistently amplified regions seen in all MGTs examined were present in 54.5–81.9% of the metaphase spreads analyzed (Table 1). Amplification of chromosomal regions 1q21–22 and 7q33 include the loci for cyclin E1 (D.P., unpublished work) and c-*myc* (14), respectively (Fig. 5 *A* and *B* and Table 1). These results indicate that cyclin E1, in addition to c-*myc*, may also be amplified in E_2-induced MGTs.

Discussion

Centrosome amplification, CIN, and aneuploidy are striking features of human DCIS and BC (21, 22, 30, 14–17). Recently, we have shown that Fisher and SD female rats administered with synthetic chemical and environmental carcinogens yielded primarily diploid MGTs, whereas MGTs induced by E_2 alone in ACI rats were highly aneuploid (14). The molecular alterations reported here, in E_2-treated female ACI rat MGs and MGTs, which precede aneuploidy, are similar to those seen in early preinvasive human sporadic breast lesions and thus likely to be distinctively related to the causation of this disease. The prevention of E_2-induced MGTs in female ACI rats by the concomitant administration of tamoxifen (5) strongly indicates that the MGTs induced are driven and mediated by E via ERα. Moreover, both histological changes and the induction of ERα and progesterone receptor isoforms were also prevented by the concomitant tamoxifen treatment (5).

The high frequencies of E_2-mediated centrosome amplification observed in dysplasias, DCISs, and primary MGTs in female ACI rats reported herein link these centrosome defects to the CIN and aneuploidy in DCISs and MGTs shown previously by us (14). Furthermore, the centrosome amplification found in most but not

Table 1. Frequency of genomic alterations determined by CGH analysis in female ACI rat E_2-induced mammary tumors

Chromosome	Genetic alteration	Region*	Locus*	Ratio†	Frequency, %	*P* value‡
1	q11–q22	1q21–22	*Ccne1*	7/11	63.6	0.017
4§	q41–q44	4q32–44	*Ccnd2*	7/11	63.6	0.005
7§	q31–q33	7q33	*c-myc*	9/11	81.9	0.005
9	q11–q13			6/11	54.5	0.056
11§	p–q11			6/11	54.5	0.056
13§	q			7/11	63.6	0.017
20§	p12			9/11	81.9	0.005

Eleven individual MTs were examined with an average of 10 metaphases per MT.
*From Entrez Genome, *Ratus norvegicus* Map View (www.ncbi.nlm.nih.gov/mapview/maps.cgi).
†Frequencies ≥30%.
‡Analyzed by binomial distribution.
§Chromosomal alterations identified by karyotype analysis.

all cells within a given DCIS suggests that the development of these MGTs is clonal. Interestingly, hamster tumors in the kidney and their early tumorous lesions induced by E treatment alone also exhibited high frequencies of centrosome amplification, CIN, and aneuploidy (33, 36, 37). These molecular changes appear to be common features of E-induced oncogenic processes. Although the precise sequence of these events leading to tumor aneuploidy is unresolved (26, 38, 39), it is evident that there is an early loss of normal centrosome homeostasis, shown here, in E_2-mediated dysplasias, DCISs, and primary MGTs in female ACI rats. This process may involve the E-mediated c-*myc* overexpression and the downstream deregulation of the cell cycle (40), indicated by the overexpression of cyclin E.cdk2 and eventual amplification of c-*myc* (14). This sequence is similar to that reported by us in the E_2-induced tumors in the hamster kidney (37, 41). These data suggest there is an intimate causal relationship between the deregulation of cell cycle components and centrosome amplification, leading to CIN. Consistent with our findings, MYC protein overexpression elicits CIN and increased tumorigenicity in rat 1A cells (42). In these cells, ectopic expression of c-*myc* perturbs the coupling of DNA replication and mitosis (43). Moreover, rat 1A-Myc ER cells in the presence of E exhibited irreversible chromosomal aberrations, including numerical changes (44). Downstream, overexpression of cyclin E.cdk2, but not cyclin D1 or A, in immortalized rat embryo fibroblasts and human breast epithelial cells resulted in CIN (45).

Centrosome-associated kinases are key regulators of centrosome maturation, chromosome segregation, and cytokinesis (18, 46–48). Overexpression of Aur-A in NIH 3T3 cells has been shown to induce centrosome amplification, aneuploidy, and transformation (25). After ectopic overexpression of Aur-A in MCF-7 cells, similar changes were detected (26). These results clearly indicate that Aur-A when overexpressed behaves as an oncogene. Aur-A overexpression has been seen in 94% of 33 invasive ductal BC samples, irrespective of the histopathology type, when compared with normal ductal breast tissue (27). This finding is comparable to the frequency of Aur-A overexpression seen here in solely E_2-induced primary ACI rat MGTs. The finding that in 4-mo E_2-treated MGs, Aur-A expression, both mRNA and protein, rose to a level essentially equal to that of primary MGTs indicates that this increase is likely due to the coincident rise in DCISs found at this treatment interval. These data indicate that the high levels of Aur-A in DCISs may be a crucial event during early MGT development. Our finding is consistent with a recent report showing markedly high levels of Aur-A in human breast DCISs (49).

Although Aur-A overexpression and centrosome amplification were detected in *N*-nitrosourea-induced rat MGTs (50), the

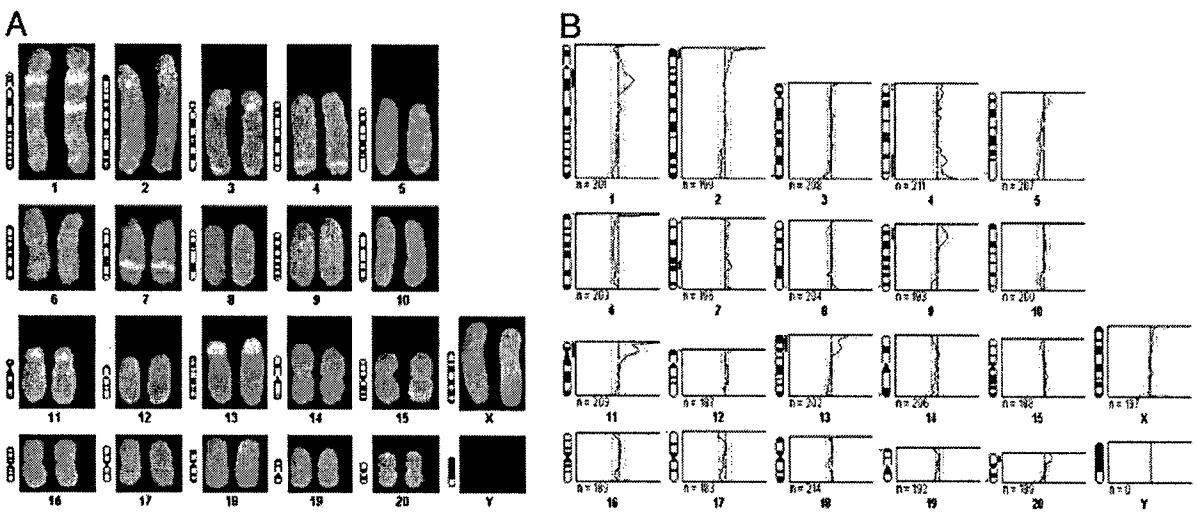

Fig. 5. CGH of an ACI rat mammary gland tumor. (*A*) Representative CGH rat spleen karyotype employing female ACI rat E_2-induced primary MGTs. DNA was detected in green (SpectrumGreen FITC, Vysis) and untreated MG DNA in red (SpectrumRed TRITC, Vysis). Note the regional gains on chromosomes 1, 3, 4, 7, 11, 13, and 20. (*B*) Ratio profiles of green-to-red fluorescence intensities after CGH from female ACI rat E_2-induced MGTs. Profiles from 11 individual MGTs were normalized to an average green-to-red ratio of 1.0. The right and left lines depict the upper and lower threshold of 1.2 for overrepresentation (copy gain) and 0.80 for underrepresentation (copy loss), respectively.

frequency of occurrence of these changes in synthetic chemical carcinogen-induced MGTs would be very low because the vast majority (>85%) of these MGT cells are diploid (14, 51, 52). It remains to be seen whether other centrosomal kinases (18, 27, 46, 48, 53, 54) might also be involved in effecting centrosome amplification in solely E_2-induced murine breast oncogenesis.

The presence of a single γ-tubulin isoform in control tissue and two γ-tubulin isoforms in E_2-treated MGs and MGTs may be due to differential posttranslational modification, as has been reported in non-mammalian species (55–57). These two γ-tubulins have been implicated in having distinct roles in nucleation, organization, and stabilization of microtubules based on their differential binding to centrosomes and to mitotic spindle poles (56). The slow γ-tubulin isoform seen in the present study in MGTs may explain the increased microtubule nucleating capacity of amplified centrosomes observed in human breast tumors (30).

The CIN and aneuploidy generated by E_2-induced ACI rat MGTs yielded both nonrandom and random chromosome changes. The consistent regional chromosome alterations detected by CGH reported here largely coincided with the numerical chromosome alterations (i.e., gains in chromosomes 7, 11, 13, 19, and 20) detected by conventional karyotype analyses, described earlier by us, for primary ACI rat MGTs (14). Remarkably, the overexpression and amplification of the c-*myc* gene was found in two distinctive tumors that have in common E as the sole etiologic agent (14, 37). Similar alterations in the c-*myc* gene have been commonly found in human breast DCISs and invasive ductal BCs (58, 59). A sequence of cascading events is proposed for ACI rat breast oncogenesis, beginning with E interacting with its receptor, ERα, followed by c-*myc*/MYC protein overexpression, subsequent cyclin E.cdk2 and Aur-A overexpression, centrosome amplification, CIN, aneuploidy, and ultimately BC. Thus, E is intimately linked for the first time to these aforementioned molecular changes leading to tumor development. These findings may provide targets for the prevention and therapeutic intervention of human sporadic BC.

This work was supported by National Institutes of Health–National Cancer Institute Grants CA87591 (to S.A.L.), CA102849 (to J.J.L.), and CA72836 (to J.L.S.) and Department of Defense Breast Cancer Research Program Grant DAMD 17-01-1-0753 (to W.L.L.).

1. King, M.-C., Rowell, S. & Love, S. M. (1993) *J. Am. Med. Assoc.* **269,** 1975–1980.
2. Clemons, M. & Gross, P. (2001) *N. Engl. J. Med.* **344,** 276–285.
3. Feigelson, H. S. & Henderson, B. E. (1996) *Carcinogenesis* **17,** 2279–2284.
4. Adami, H.-O., Persson, I., Ekbom, A., Wolk, A., Ponten J. & Trichopoulas, D. (1995) *Mutat. Res.* **333,** 29–35.
5. Li, S. A., Weroha, S. J. & Li, J. J. (2002) *J. Endocrinol.* **175,** 297–305.
6. Blankenstein, M. A., Broerse, J. J., deVries, J. B., vandenBerg, K. K., Knaan, S. & van der Molen, H. J. (1977) *Eur. J. Cancer* **13,** 1437–1443.
7. Daling, J. R., Malone, K. E., Doody, D. R., Voigt, L. F., Bernstein, L., Coates, R. J., Marchbanks, P. A., Norman, S. A., Weiss, L. K., Ursin, G., *et al.* (2002) *Cancer* **95,** 2455–2464.
8. Li, C. I., Weiss, N. S., Stanford, J. L. & Daling, J. R. (2000) *Cancer* **88,** 2570–2577.
9. Colditz, G. A., Stampfer, M. J., Willett, W. C., Hennekens, C. H., Rosner, B. & Speizer, F. E. (1990) *J. Am. Med. Assoc.* **264,** 2648–2653.
10. Chetrite, G. S., Cortes-Prieto, J., Philippe, J. C., Wright, F. & Pasqualini J. R. (2000) *J. Steroid Biochem. Mol. Biol.* **72,** 23–27.
11. Vermeulen, A., Deslypere, J. P., Paridaens, R., LeClereq, G., Roy, F. & Heuson, J. C. (1986) *Eur. J. Cancer* **22,** 515–525.
12. Thijssen, J. H. H. & Blankenstein, M. A. (1989) *Eur. J. Cancer Clin. Oncol.* **25,** 1933–1959.
13. Thijssen, J. H. H., van Landeghem, A. A. J. & Poortman, J. (1986) *Ann. N.Y. Acad. Sci.* **484,** 106–116.
14. Li, J. J., Papa, D., Davis, M. F., Weroha, J. S., Aldaz, C. M., El-Bayoumy, K., Ballenger, J., Tawfik, O. & Li, S. A. (2002) *Mol. Carcinog.* **3,** 56–65.
15. Arnerlov, C., Emdin, S. O., Cajander, S., Bengtsson, N.-O., Tavelin, B. & Roos, G. (2001) *Anal. Cell. Pathol.* **23,** 21–28.
16. Makris, A., Allred, D. C., Powles, T. J., Dowsett, M., Fernando, I. N., Trott, P. A., Ashley, S. E., Ormerod, M. G., Titley, J. C. & Osborne, C. K. (1997) *Breast Cancer Res. Treat.* **44,** 65–74.
17. Leal, C. B., Schmitt, F. C., Bento, M. J., Maia, N. C. & Lopez, C. S. (1995) *Cancer* **75,** 2123–2131.
18. Dutertre, S., Descamps, S. & Prigent, C. (2002) *Oncogene* **21,** 6175–6183.
19. Kramer, A., Neben, K. & Ho, A. D. (2002) *Leukemia* **16,** 767–775.
20. Pihan, G. A., Wallace, J., Zhou, Y. & Doxsey, S. J. (2003) *Cancer Res.* **63,** 1398–1404.
21. Lingle, W. L., Barrett, S. L., Negron, V. C., D'Assoro, A. B., Boeneman, K., Liu, W., Whitehead, C. M., Reynolds, C. & Salisbury, J. L. (2002) *Proc. Natl. Acad. Sci. USA* **99,** 1978–1983.
22. D'Assoro, A. B., Lingle, W. L. & Salisbury, J. L. (2002) *Oncogene* **21,** 6146–6153.
23. Salisbury, J. L. (2001) *J. Mamm. Gland Biol. Neoplasia* **6,** 203–212.
24. Katayama, H., Brinkley, W. R. & Sen, S. (2003) *Cancer Met. Rev.* **22,** 451–464.
25. Brinkley, B. R., Goepfert, T. M. (1998) *Cell Motil. Cytoskeleton* **41,** 281–288.
26. Zhou, H., Kuang, J., Xhow, L., Kuo, W. L., Gray J. W., Suhin, A., Brinkley, B. R. & Sen, S. (1998) *Nat. Genet.* **20,** 189–193.
27. Miyoshi, Y., Iwao, K., Egawa, C. & Noguchi, S. (2001) *Int. J. Cancer* **92,** 370–373.
28. Tanaka, T., Kimura, M., Matsunaga, K., Fukada, D., Mori, H. & Okano, Y. (1999) *Cancer Res.* **59,** 2041–2044.
29. Errabolu, R., Sanders, M. A. & Salisbury, J. L. (1994) *J. Cell Sci.* **107,** 9–16.
30. Lingle, W. L., Lutz, W. H., Ingle, J. N., Maihle, N. J. & Salisbury, J. L. (1998) *Proc. Natl. Acad. Sci. USA* **96,** 214–219.
31. Carroll, P. E., Okuda, M., Horn, H. F., Biddinger, P., Stambrook, P. J., Gleich, L. L., Li, Y. Q., Tarapore, P. & Fukasawa, K. (1999) *Oncogene* **18,** 1935–1944.
32. Gemmell, N. J. & Akyiama, S. (1996) *Trends Genet.* **12,** 338–339.
33. Papa, D., Li, S. A. & Li, J. J. (2003) *Mol. Carcinog.* **38,** 97–105.
34. Kallioniemi, A., Kallioniemi, O.-P. & Piper, J. (1994) *Genes Chromosomes Cancer* **10,** 231–243.
35. Mohapatra, G., Kim, D. H. & Feuerstein, B. G. (1995) *Genes Chromosomes Cancer* **13,** 86–93.
36. Li, J. J., Weroha, S. J., Davis, M. F., Hou, X., Tawfik, O. & Li, S. A. (2001) *Endocrinology* **142,** 4006–4014.
37. Li, J. J., Hou, X., Banerjee, S. K., Liao, D. J., Maggouta, F., Norris, J. S. & Li, S. A. (1999) *Cancer Res.* **59,** 2340–2346.
38. Salisbury, J. L., Whitehead, C. M., Lingle, W. L. & Barrett, S. L. (1999) *Biol. Cell* **91,** 451–460.
39. Li, R., Sonik, A., Stindl, R., Rasnick, D. & Duesberg, P. (2000) *Proc. Natl. Acad. Sci. USA* **97,** 3236–3241.
40. Weroha, J. S. (2004) *Proc. Am. Assoc. Cancer Res.* **45,** 12.
41. Liao, D. J., Hou, X., Bai, S., Li, S. A. & Li, J. J. (2000) *Carcinogenesis* **21,** 2167–2173.
42. Felsher, D.W. & Bishop, J. M. (1999) *Proc. Natl. Acad. Sci. USA* **96,** 3940–3944.
43. Li, Q. & Dang, C. V. (1999) *Mol. Cell. Biol.* **19,** 5339–5351.
44. Mai, S., Fluri, M., Siwarski, D. & Hupp, I. (1996) *Chromosome Res.* **4,** 365–371.
45. Spruck, C. H., Won, K.-A. & Reed, S. I. (1999) *Nature* **401,** 297–300.
46. Nigg, E. A. (2001) *Nat. Rev. Mol. Cell Biol.* **2,** 21–32.
47. Warner, S. L., Bearss, D. J., Han, H. & Von Hoff, D. D. (2003) *Mol. Cancer Ther.* **2,** 589–595.
48. Carmena, M. & Earnshaw, W. C. (2003) *Nat. Rev. Mol. Cell Biol.* **4,** 842–854.
49. Hoque, A., Carter, J., Xia, W., Hung, M. C., Sahin, A. A., Sen, S. & Lippman, S. M. (2003) *Cancer Epidemiol. Biomarkers Prev.* **12,** 1518–1522.
50. Goepfert, T. M., Adigum, Y. E., Zhong, L., Gay, J., Medina, D. & Brinkley, W. R. (2002) *Cancer Res.* **62,** 4115–4122.
51. Aldaz, C. M., Gollahon, L. S. & Chen, A. (1992) *Prog. Clin. Biol. Res.* **376,** 137–153.
52. Haag, J. D., Hsu, L. C., Newton, M. A. & Gould, M. N. (1996) *Mol. Carcinog.* **17,** 134–143.
53. Smith, M. R., Wilson, M. L., Hamanaka, R., Chase, D., Kung, H., Longo D. L. & Ferris, D. K. (1997) *Biochem. Biophys. Res. Commun.* **234,** 397–405.
54. Fry, A. M. (2002) *Oncogene* **21,** 6184–6194.
55. Oakley, C. E. & Oakley, B. R. (1989) *Nature* **338,** 662–664.
56. Lajoie-Mazenc, I., Detraves, C., Rotaru, V., Gares, M., Tollon, Y., Jean, C., Julian, M., Wright, M. & Raynaud-Messina, B. (1996) *J. Cell Sci.* **109,** 2483–2492.
57. Starita, L. M., Machida, Y., Sankaran, S., Elias, J. E., Griffin, K., Schlegel, B. P., Gygi, S. P. & Parvin, J. D. (2004) *Mol. Cell. Biol.* **24,** 8457–8466.
58. Hynes, N. E. & Lane, H. A. (2001) *J. Mamm. Gland Biol. Neoplasia* **6,** 141–150.
59. Deming, S. L., Nass, S. J., Dickson, R. B. & Trock, B. J. (2000) *Br. J. Cancer* **83,** 1688–1695.

JBC Papers in Press. Published on October 26, 2004 as Manuscript M407105200

Short-term cyclin D1 overexpression induces centrosome amplification, mitotic spindle abnormalities, and aneuploidy

Christopher J. Nelsen,[1,2] Ryoko Kuriyama,[3,4] Betsy Hirsch,[4,5] Vivian C. Negron,[6] Wilma L. Lingle,[6] Melissa M. Goggin,[2] Michael W. Stanley,[7] and Jeffrey H. Albrecht[1,2,4*]

From the [1]Division of Gastroenterology, Hennepin County Medical Center, Minneapolis, MN 55415; the [2]Minneapolis Medical Research Foundation, Minneapolis, MN 55404; the [3]Department of Genetics, Cell Biology, and Development, University of Minnesota, Minneapolis, MN 55455; the [4]University of Minnesota Cancer Center, Minneapolis, MN 55455; the [5]Department of Laboratory Medicine and Pathology, University of Minnesota, Minneapolis, MN 55455; the [6]Division of Experimental Pathology, Tumor Biology Program, Mayo Clinic, Rochester, MN 55905; and the [7]Department of Pathology, Hennepin County Medical Center, Minneapolis, MN 55415.

*To whom correspondence should be addressed: Division of Gastroenterology (G5), Hennepin County Medical Center, 701 Park Avenue, Minneapolis, MN 55415. Phone: (612) 873-8582. Fax: (612) 904-4366. E-mail: albre010@tc.umn.edu.

Running title: Cyclin D1 induces centrosome amplification and aneuploidy

This work was supported by NIH award DK54921 and a special grant from the University of Minnesota Cancer Center.

Summary

In normal cells, cyclin D1 is induced by growth factors and promotes progression through G1 phase of the cell cycle. Cyclin D1 is also an oncogene that is thought to act primarily by bypassing the requirement for mitogens during G1 phase. Studies of clinical tumors have found that cyclin D1 overexpression is associated with chromosome abnormalities, although a causal effect has not been established in experimental systems. In this study, we found that transient expression of cyclin D1 in normal hepatocytes *in vivo* triggered dysplastic mitoses, accumulation of supernumerary centrosomes, abnormalities of the mitotic spindle, and marked chromosome changes within several days. This was associated with upregulation of checkpoint genes p53 and p21 as well as hepatocyte apoptosis in the liver. Transient transfection of cyclin D1 also induced centrosome and mitotic spindle abnormalities in breast epithelial cells, suggesting that this may be a generalized effect. These results indicate that cyclin D1 can induce deregulation of the mitotic apparatus and aneuploidy, effects that could contribute to the role of this oncogene in malignancy.

Introduction

A critical component of normal cell division is the accurate distribution of chromosomes and other cellular components during mitosis. Abnormal cell division and chromosome content are hallmarks of cancer and are associated with a poor prognosis in a number of tumors (1,2). The mechanisms by which cells acquire chromosome changes have not been fully identified, but alterations of centrosomes and the mitotic spindle apparatus appear to play an important role (3-6). Most normal cells contain one centrosome, which serves as the major microtubule organizing center and participates in processes such as cell polarity, migration, and intracellular transport (3-7). In normal cell division, centrosomes undergo one round of duplication in a manner analogous to the replication of chromosomal DNA during S phase. During mitosis, centrosomes direct the formation of bipolar mitotic spindles that assure equal segregation of chromosomes between daughter cells.

Increased numbers of centrosomes are frequently observed in malignant cells (3-7). This is thought to result in distortion of the mitotic apparatus and abnormal sorting of chromosomes during cell division. The resulting changes in chromosome compliment can lead to loss of tumor suppressor genes or gain of oncogene function that further promote the malignant phenotype. In addition to changes in centrosome number, alterations in the centrioles and pericentriolar material that make up the centrosome are frequently seen in cancers. Although recent studies have provided substantial insight into the proteins that make up the centrosome, the identity and function of centrosome components, and their potential derangement in cancer, remain to be fully characterized.

Recent studies have identified proteins that govern the centrosome duplication cycle (reviewed in (5,7-11)). The activity of cyclin-dependent kinase (cdk) 2 is thought to be required for centrosome duplication in tissue culture and cell-free systems. Relevant substrates of cdk2 include the Mps1 kinase, nucleophosmin/B23, and CP110, which regulate centrosome duplication. The cdk inhibitor p21, which is a downstream target of p53, is thought to inhibit the centrosome cycle through inactivation of cdk2 activity. Cells lacking p53 function may also be deficient in other cellular checkpoint mechanisms that affect centrosome duplication. In addition to p53 and p21, mutations of tumor suppressor genes Brca1, Brca2, Gadd45, and adenomatous polyposis coli are associated with centrosome abnormalities. Conversely, overexpression of several oncogenes that regulate the mitotic spindle apparatus, such as Ran and Aurora-A, can disrupt normal centrosome function.

Cyclin D1 is a G1 phase regulatory protein that promotes physiologic cell proliferation downstream of mitogens and other extracellular stimuli (12-14). In addition, cyclin D1 is a putative oncogene that is overexpressed in many human malignancies. Constitutive expression of cyclin D1 is likely to contribute to malignant transformation by reducing the dependency on extracellular signals that normally control proliferation – that is, it diminishes the requirement for mitogens in the transition through the G1 restriction point. Studies of clinical tumors have found that cyclin D1 overexpression is associated with chromosomal abnormalities (15-18), although data indicating that cyclin D1 can cause mitotic or chromosome abnormalities is lacking. In this manuscript, we document that transient cyclin D1 expression induced centrosome amplification, deregulation of the mitotic spindle, and overt chromosome abnormalities within a matter

of days. These results suggest that cyclin D1 may promote malignancy by causing genomic instability.

Experimental Procedures

Animals - All animal studies were completed following IACUC approved techniques and NIH guidelines. Eight week old male Balb/C (Harlan Sprague-Dawley), or p21-/- or p21+/+ (Jackson labs) mice were injected with 5 x 10^9 plaque-forming units via tail vein injection of E1-deleted recombinant adenoviruses encoding cyclin D1, cyclin E, or β-galactosidase (control) as previously described, followed by liver harvest and processing (19-22). The construction of the cyclin D1 (ADV-D1) and cyclin E (ADV-E) adenoviruses is described in prior manuscripts (19,23,24); the control adenovirus is equivalent except for the encoded transgene.

Cell Culture and Immunohistochemistry - Mouse hepatocytes were isolated using Liver Perfusion Media and Liver Digest Media (Invitrogen). Cells were purified through a Percoll gradient and cultured for indicated times on collagen treated glass coverslips in Williams E media in the presence of EGF (10 ng/ml) and insulin (20 milliunits/ml) (23). Media was changed daily; colchemid (25 ng/ml) was added 3 hours prior to fixation. Immunohistochemistry was completed on coverslips with attached cells after being fixed in –20 C methanol and then rehydrated in PBS containing 0.05% Tween-20. A mixture of primary antibodies, mouse monoclonal anti-α-tubulin (Sigma-Aldrich) and rabbit polyclonal anti-Cep135, or anti-Cep135 and anti-centrin (gift of Dr. J. Salisbury) were incubated as previously described (25,26). hMEC cells were incubated

with monoclonal anti-α-tubulin and rabbit polyclonal anti-γ-tubulin (Sigma-Aldrich) (6,27). Appropriate secondary antibodies were used to visualize staining. Microscopic identification was completed using a Nikon eclipse microscope with epifluorescence optics or a Zeiss LSM 510 confocal microscope. In Figure 2E, slides were stained with DAPI and the percent of cells in metaphase was counted in three different specimens for each condition.

Apoptosis and Flow Cytometry - TUNEL staining on formalin-fixed liver tissue sections was performed using the ApoTag (Intergen) kit following the manufacturer's instructions, as previously described (19). Flow cytometry was completed using previously described methods (19,21).

Quantification of p21 and p53 mRNA by Real-Time PCR (RT-PCR) - Total RNA from each liver was isolated as previously described (28). RNA samples were subjected to agarose gel electrophoresis and visualized using ethidium bromide to ensure that the RNA was not grossly degraded. Samples of RNA (5 μg) were treated with DNAse I (DNA-free™, Ambion) according to the manufacturer's instructions. Oligo dT primed cDNA was generated from 4 μg of each RNA with Taqman reverse transcriptase reagent kit (Applied Biosystems). Mouse p21 DNA sequences for upper (5'-cggtggaactttgacttcgt-3') and lower (5'- cagggcagaggaagtactgg-3') primers, p53 upper (5'-agagaccgccgtacagaaga-3') and lower (5'-ctgtagcatgggcatccttt-3') primers, and β–actin sequences for upper (5'-aaccctaaggccaaccgtgaaaag-3') and lower (5'-accgctcgttgccaatagtgatga-3') primers were selected using the Primerselect program (DNASTAR, Inc., Madison). The resulting sequences were synthesized in the University of Minnesota microchemical facility and purified by HPLC. RT-PCR was completed

using a LightCycler FastStart DNA Master SYBR Green I Kit (Roche Molecular Biochemicals). Samples were denatured for 10 min at 95 °C, and then 40 cycles of 95 °C for 20 s, 60 °C for 20 s, and 68 °C for 20 s. Optimization of $MgCl_2$ and primer concentrations were completed as recommended by the manufacturer (2.4 mM $MgCl_2$ for p21 and p53 and 3 mM for β–actin). Primer concentrations were found to be optimal at 0.2 μM for p21 and p53 and 0.1 μM for β–actin. For each mRNA, quantification was completed by comparison (linear interpolation) of the cycles to saturation in each sample. p21 and p53 mRNA were normalized to β–actin mRNA expression (which did not change under any of the conditions, data not shown), and the relative amounts were determined as recommended by the manufacturer.

Transfection of Human Mammary Epithelial cells (hMEC) - hMEC cells were transfected with the cyclin D1 or control adenoviruses (25 plaque-forming units per cell), seeded on glass coverslips, and harvested at 48 h as previously described (27).

Results

Persistent expression of cyclin D1 promotes abnormal hepatocyte mitoses in vivo - Previous studies have suggested that cyclin D1 plays an important role in regulating hepatocyte proliferation in response to extracellular stimuli (21-23,29-31). In normal liver, hepatocytes rarely replicate, but these cells rapidly enter the cell cycle in response to injuries that diminish functional hepatic mass (31,32). We have found that transient transfection of hepatocytes *in vivo* with a recombinant adenovirus expressing human cyclin D1 (ADV-D1) is sufficient to trigger hepatocyte replication and liver

growth under conditions where these cells are normally quiescent (20-22). Intravenously injected replication-defective (E1-deleted) adenoviruses such as these primarily target the liver and can transfect >95% of hepatocytes; this system has been used extensively to study the effect of transient single-gene expression in these cells (24,33-35). At two days after cyclin D1 transfection, hepatocyte mitoses appeared normal (Fig. 1). However, at six days the mitotic figures were uniformly abnormal, with multipolar mitoses and apparently asymmetric segregation of chromatin. Such features are commonly seen in neoplasia. Injection with the control adenovirus did not induce significant cell cycle progression, and the few observed mitoses were morphologically normal (data not shown and ref. (20)). Furthermore, mitoses observed at 48 hours after partial hepatectomy did not display similar abnormalities (data not shown). Thus, protracted cyclin D1 expression (over a matter of days) led to apparent deregulation of the mitotic apparatus, which is a likely precursor of aneuploidy (1-4). Because this suggests a novel mechanism by which cyclin D1 could promote neoplasia, we examined the mitotic and chromosome abnormalities in greater detail.

Cyclin D1 triggers centrosome amplification and aberrant mitotic spindles in hepatocytes - To further explore the derangement of hepatocyte mitosis by cyclin D1, we examined the regulation of centrosome number and mitotic spindle structure using established immunohistochemical techniques. The study of centrosomes and mitotic spindles in fixed tissue specimens is limited by technical considerations (36). We therefore transfected mice with ADV-D1 (or the control vector) for three days and then isolated hepatocytes by collagenase perfusion. The cells were placed in culture for two days in the presence of EGF and insulin, which triggers proliferation of quiescent

hepatocytes. Cells were then fixed and co-immunostained with antibodies to centrosome proteins (Cep-135 or γ-tubulin) and α-tubulin, which is the major mitotic spindle protein (4,25,26,36). All γ-tubulin-positive foci also stained with Cep-135 (data not shown), and we therefore elected to use Cep-135 as the marker of centrosomes in hepatocytes because of the quality of the antibody (26).

In normal hepatocytes, or those transfected with the control adenovirus, we observed bipolar mitotic spindles with either two or four centrosomes (Fig. 2A), reflecting the normal population of 2N and binucleated (2 X 2N) cells in the liver (37). Similarly, hepatocytes transfected with a recombinant adenovirus encoding human cyclin E (ADV-E) did not demonstrate substantially increased centrosome numbers or abnormal mitotic morphology. In contrast, cyclin D1-transfected hepatocytes uniformly demonstrated irregular multipolar mitotic spindles with supernumerary centrosomes. The number of centrosomes (as defined by distinct Cep-135 or γ-tubulin-positive foci) exceeded the number of spindle poles, because several centrosomes sometimes clustered at a single pole (Fig. 2A, inset). As shown in Fig. 2B, cyclin D1-transfected hepatocytes almost always contained more than four centrosomes, and some had ≥ 20 per cell. Thus, at five days after cyclin D1 transfection (three days *in vivo* and two days in culture), hepatocytes demonstrated substantially increased centrosome numbers and markedly abnormal mitotic morphology.

Normal centrosomes consist of a pair of centrioles surrounded by pericentriolar material (5). Centrosomes are typically visualized and quantified by performing immunostaining for pericentriolar proteins such as γ-tubulin or Cep135. In Fig. 2C, cells were immunostained with an antibody to centrin, a centriolar protein, which is frequently

used to visualize these structures (3,36). As expected, in both normal and cyclin D1-transfected cells, centrosomes staining with Cep-135 showed two centrin-positive centrioles. These results indicate that cyclin D1 led to hyperamplification of centrosomes with a normal number of centrioles.

The number of centrosomes per cell has been linked to DNA content, and one potential mechanism of centrosome hyperamplification is aborted cell division that gives rise to polyploid cells with increased centrosome numbers (5,38). To examine the relationship of cell ploidy to centrosome number, cells were subjected to FACS analysis to examine DNA content (Fig. 2D). Normal or control-transfected hepatocytes demonstrated clear 2N and 4N peaks. Cyclin D1-transfected hepatocytes showed the same peaks, with proportionately more 4N cells and a substantial number of 8N cells. However, a significant number of cells did not fall into the 2N, 4N, or 8N peaks, suggesting that cyclin D1 induced aneuploidy (see below). Furthermore, very few cells with > 8N DNA content were observed. In the cyclin D1-transfected cells, centrosome content (Fig. 2B) appeared to be increased to a greater degree than DNA content (Fig. 2D). Thus, persistent cyclin D1 expression may lead to uncoupling of the centrosome cycle from the cell cycle.

Normal hepatocytes proliferate readily in culture in the presence of appropriate growth factors, and previous studies have shown that cyclin D1 is induced in these cells in a mitogen-dependent manner (23,29,31). In Figure 2E, slides were stained with DAPI and the number of cells displaying metaphase morphology was found to be similar in cyclin D1-transfected or control cells. Therefore, it is apparent that re-entry into the cell cycle *per se* was not sufficient to cause the observed centrosome and mitotic

abnormalities. Interestingly, cyclin D1 induced the accumulation of supernumerary centrosomes even in interphase cells (Fig. 3), whereas control-transfected or normal cells showed 2-4 centrosomes (data not shown). As was the case for the metaphase cells, the number of centrosomes in cyclin D1-transfected interphase cells did not seem to clearly correlate with the DNA content as assessed by FACS analysis (Fig. 2D). Thus abnormal centrosome numbers were observed in the majority of cyclin D1-transfected cells.

To further examine the relationship between cell ploidy and centrosome number, we studied hepatocytes two days following transfection with cyclin D1 (24 hr *in vivo* and 24 hr in culture, Fig. 4). At this early time point, the mitotic cells had bipolar spindles after cyclin D1 transfection (Fig. 4A; also see Fig. 1). However, many cells showed a substantially increased number of centrosomes (Fig. 4B), which clustered at the two spindle poles (Fig. 4A). FACS analysis indicated that there was a shift to 4N DNA content and a portion of cells had >4N content (Fig. 4C). However, few cells had 8N content, and the large number of centrosomes seen in some cells (Fig. 4B) was not accompanied by a proportional increase in DNA content. These studies further suggest that cyclin D1 can differentially regulate centrosome number and cell cycle progression. These results also indicate that although short-term cyclin D1 overexpression can promote both processes, centrosome overduplication and multipolar spindle formation may be distinctly regulated at early time points.

Cyclin D1 induces chromosomal abnormalities in hepatocytes - The data shown above indicates that over a period of several days, cyclin D1 induced abnormal mitoses, suggesting the possibility that it may also affect the cellular chromosome content. The FACS data in Figures 2D and 4C indicated that a substantial portion of cyclin D1-

transfected cells contained hyperploid nuclei that did not correspond with the 2N, 4N, or 8N peaks, suggesting that cells with grossly abnormal chromosome content were present. To examine this further, chromosome morphology from control and transfected hepatocytes was evaluated using standard techniques (Fig. 5A). In normal and control-transfected cells, $\geq$ 88% of cells contained the expected 2N, 4N, or 8N chromosome compliment. On the other hand, in cyclin D1-transfected cells, only 32% of cells fell within these peaks. The combined data from the FACS analysis and chromosome morphology data indicate that cyclin D1 induces polyploidy and the accumulation of cells with grossly abnormal chromosome content that does not fall within the predicted 2N, 4N and 8N peaks.

To further examine the effect of cyclin D1 on chromosome integrity, mitotic spreads were evaluated for the presence of overt structural abnormalities. As is shown in Fig. 5B, cyclin D1 promoted the development of chromosome breaks, free centromeres, and dicentric chromosomes. More than 20% of cyclin D1-transfected hepatocytes demonstrated such abnormalities (Fig. 5C). These data indicate that short-term cyclin D1 transfection leads to both numerical and structural chromosome abnormalities in hepatocytes.

The induction of mitotic and chromosome abnormalities by cyclin D1 is accompanied by apoptosis - In response to injuries that promote abnormalities of the mitotic spindle or DNA damage, normal cells activate checkpoint mechanisms that inhibit cell cycle progression or induce apoptosis (5,7,10). In addition, cells with severe aneuploidy can undergo apoptosis due to "chromosomal insufficiency" (4). To examine whether similar mechanisms were activated following cyclin D1 transfection in our

system, we evaluated liver specimens for the presence of apoptosis. As is shown in Fig. 6, at 6 days following cyclin D1 transfection, a substantial number of hepatocytes were overtly apoptotic as determined by TUNEL staining. These data suggest that the mitotic and chromosome abnormalities induced by cyclin D1 resulted in activation of checkpoint mechanisms that triggered hepatocyte apoptosis.

Protracted cyclin D1 expression leads to marked induction of p53 and p21 gene expression - In our prior studies, we found that transfection with ADV-D1 led to activation of cyclin/cdk complexes, robust proliferation, and numerous mitotic figures within 1-2 days (20-22). At 6 days after transfection, despite continued expression of cyclin D1, cyclin D1/cdk4 and cyclin E/cdk2 complexes were relatively inhibited and the rates of DNA synthesis and mitosis were relatively diminished compared to 1-2 days (although each of these parameters were still up-regulated compared to normal or control-transfected livers) (20). This suggests that prolonged expression of cyclin D1 induced antiproliferative signals that suppress cyclin/cdk activity and cell cycle progression; our previous data indicated that marked induction of the cdk-inhibitory protein p21 might play a role in this response (20). At the 6 day time point, we speculated that the induction of p21 was due in part to the activation of checkpoint mechanisms that respond to chromosome and/or mitotic spindle abnormalities. Studies in other systems would predict that p53 may be involved in these checkpoints, and can induce both p21 expression and apoptosis (7,10). To examine the potential involvement of p21 and p53 in our system, we evaluated the expression of these genes by RT-PCR (Fig. 7). As previously shown, cyclin D1 induced p21 at 1 day after transfection, presumably as part of the normal cell cycle program. At 6 days after transfection, despite diminished cyclin D1/cdk4 activity (20),

p21 mRNA was induced to much higher levels. Furthermore, p53 mRNA was also markedly induced at 6 days. These studies suggest that the mitotic and chromosome abnormalities induced by protracted cyclin D1 expression may promote checkpoint mechanisms involving p53 and p21.

Previous studies have documented that p21 plays a role in regulating centrosome number in response to other stimuli, presumably by modulating cdk activity (5,7,10). To determine whether p21 similarly regulated the development of supernumerary centrosomes following cyclin D1 expression, we examined the response in p21-/- mice. Using the conditions outlined in Fig. 2, cyclin D1 induced an average of 14.63 +/- 4.75 centrosomes in hepatocytes isolated from p21-/- mice as compared to 8.48 +/- 3.63 centrosomes in matched wild-type mice. This suggests that the marked induction of p21 in response to cyclin D1 overexpression moderately diminishes the accumulation of supernumerary centrosomes.

Centrosome abnormalities persist for months after cyclin D1 transfection - Our data indicate that the induction of mitotic and chromosome abnormalities by cyclin D1 is associated with both a cell cycle arrest and apoptosis. This suggests that the hepatocytes activated normal checkpoint mechanisms that could result in the elimination of abnormal cells. Previous studies have shown that first-generation recombinant adenoviruses, such as those used in our studies, promote gene expression that lasts several weeks. In our previous studies, we found that cyclin D1 expression was no longer detectable one month following transfection (20). To examine whether centrosome abnormalities persisted after cyclin D1 was no longer expressed, we examined hepatocytes 4 months after cyclin D1 transfection. As shown in Fig. 8, normal or control-transfected mice contained 2-4

centrosomes, in a pattern similar to that seen in younger mice (Fig. 2). On the other hand, 13% of cyclin D1-transfected hepatocytes contained >4 centrosomes. Thus, no hepatocytes with massively increased centrosome number (as seen at early time points after transfection) were observed in the mice 4 months after transfection. This suggests that the most abnormal cells were eliminated by the activation of normal checkpoint mechanisms. However, a portion of cells retained abnormal centrosome number, indicating that transient overexpression of cyclin D1 led to long-lasting changes in the mitotic apparatus in some cells.

Cyclin D1 induces centrosome and mitotic spindle abnormalities in breast epithelial cells - The studies described above suggest that persistent expression of cyclin D1 promotes accumulation of supernumerary centrosomes and aneuploidy in hepatocytes. To determine whether cyclin D1 might have a similar effect in other cells, we transfected human mammary epithelial cells with the cyclin D1 or control adenoviruses and examined centrosome and mitotic spindle morphology (Fig. 9) (27). Previous studies have shown that centrosome amplification occurs frequently in breast carcinoma and correlates with the degree of aneuploidy (6). As is shown in Fig. 9, after 2 days cyclin D1 induced abnormal centrosome numbers and mitotic spindle morphology. These studies suggest that cyclin D1, which is thought to play an important role in breast cancer (13,39), may contribute to the development of centrosome and mitotic abnormalities seen in these tumors.

Discussion

Cyclin D1 is thought to play an important role in the development of cancer in many organs including the liver (12-14,40,41). Constitutive overexpression of cyclin D1 is likely to contribute to the development of malignancy by reducing the dependency on mitogens and other extracellular signals that are normally required to promote progression through the late G1 restriction point (12-14). However, current models suggest that overexpression of cyclin D1 alone is not sufficient to account for carcinogenesis; additional genetic changes are required in order for cells to acquire a malignant phenotype (42). The studies outlined here indicate that transient cyclin D1 overexpression has dramatic effects on centrosome number, the mitotic apparatus, and chromosome integrity. These results suggest an additional mechanism by which cyclin D1 may promote malignant progression.

The most clearly defined role of cyclin D1 is activation of the cdk4 and cdk6 kinases in late G1 phase, which result in phosphorylation of Rb and transcription of E2F-dependent genes required for S phase (12). The cyclin D1/cdk4 complex also sequesters cdk inhibitors such as p21 or p27, thereby promoting activation of cyclin/cdk complexes acting downstream in the cell cycle. Cyclin D1 has been implicated in other cellular processes including transcriptional control, ribosome biogenesis, cell growth, differentiation, apoptosis, adhesion, and motility (12,43). In addition, clinical studies suggest that overexpression of cyclin D1 is associated with chromosome abnormalities in several different cell types (15-18). However, it is difficult to determine from these clinical studies whether cyclin D1 overexpression is a cause or a result of genomic instability, since the *cyclin D1* locus is prone to rearrangements and amplification (12).

Indirect evidence that cyclin D1 can cause genetic alterations comes from transgenic mice with constitutive expression of this protein in various organs, which leads to the development of cancer after a delay of many months (12,13,40). This suggests that over time, persistent cyclin D1 expression may contribute to the "mutator phenotype" that results in the acquisition of specific genetic abnormalities during the process of carcinogenesis (1,2,42). In addition, the marked mitotic abnormalities seen in this study suggest that overexpression of cyclin D1 may predispose to widespread random aneuploidy that underlies the "aneuploidy-cancer theory," which holds that malignancy is induced by the abnormal dosage a large number of genes (44). Notably, transgenic mice with hepatic cyclin D1 expression were noted to have aberrant hepatocyte mitotic figures prior to the development of frank malignancy, suggesting that abnormalities of the mitotic apparatus were induced early during the oncogenic process (40). However, to our knowledge, previous experimental studies have not found that cyclin D1 overexpression induces centrosome aberrations and chromosome instability.

Although genetic studies have not unequivocally demonstrated that alterations in centrosome numbers cause aneuploidy, centrosome abnormalities are observed in a wide variety of human malignancies and have been correlated with chromosome instability (reviewed in (3-6)). The factors that promote centrosome accumulation in malignant cells have not been defined, but several mechanisms have been proposed (5,10,38). One possibility is that cells fail to undergo cytokinesis, leading to both polyploidy and accumulation of extra centrosomes. According to this model, an increased number of centrosomes should be linked to chromosome content. A second possibility is that the centrosome duplication cycle becomes uncoupled from DNA replication. Other potential

mechanisms include cell fusion and the *de novo* formation of centrosomes. These possibilities are not necessarily mutually exclusive and each may be operative under certain circumstances (5). Regardless of the mechanisms involved, centrosome aberrations are likely to contribute to chromosome instability in human tumors (3-6).

Normal hepatocytes have been shown to regulate mitosis distinctly from typical models (37). As the animal ages, increasing numbers of binucleated cells and polyploid nuclei (4N and 8N) are observed. Binucleated hepatocytes appear to result from a failure of cytokinesis at the end of mitosis (37). At the time of cell division, binucleated cells contain four centrosomes that cluster into two spindle poles, resulting in a bipolar spindle apparatus that produces two 4N cells (an example of this is shown in the control-transfected cell in Fig. 4A). In the current studies, we found that at early time points after cyclin D1 transfection, hepatocytes displayed bipolar mitotic spindles despite overduplication of centrosomes (Figs. 1 and 4). Thus, like normal binucleated hepatocytes, extra centrosomes cluster at two spindle poles during the initial phase of cyclin D1 overexpression. This suggests that spindle pole formation is regulated distinctly from centrosome number, as has been suggested in other systems (5,37). However, at 6 days, when centrosome number was greatly increased, cells consistently displayed multipolar mitoses as well as chromosome abnormalities. We also found that the increase in centrosome number triggered by cyclin D1 did not clearly parallel the corresponding increase in DNA content. The rapid induction of centrosome overduplication (within 48 hours), along with the observation that centrosome number did not seem closely linked to ploidy, suggests that the abnormalities were not simply a result of failure of cytokinesis and polyploidy. The data suggest that persistent expression

of cyclin D1 can promote centrosome duplication out of proportion to cell cycle progression. However, additional studies will be required to unravel the relationship between cyclin D1, cell cycle progression, centrosome number, spindle pole formation, and aneuploidy.

This study did not directly address the mechanism(s) by which cyclin D1 may regulate centrosome accumulation. Cyclin D1 transfection induces cell cycle progression and downstream cell cycle mediators including cyclin E/cdk2 and cyclin A/cdk2 in hepatocytes (20,23). These complexes are known to promote centrosome duplication and phosphorylation of several different centrosome proteins (5,8,9). Thus, cyclin D1 may act by promoting activation of cdk2, which in turn induces centrosome and mitotic spindle abnormalities, resulting in aneuploidy. Interestingly, transfection with cyclin E alone did not promote marked centrosome abnormalities in our system. This may be due to the fact that cyclin E transfection does not induce activation of cyclin E/cdk2 or cell cycle progression in hepatocytes, presumably because these cells contain sufficient monomeric p27 to inhibit these complexes (19,45). Further studies will be required to determine whether cyclin D1 acts directly on centrosome targets, or whether it mediates effects by activating downstream cell cycle genes.

Our results differ from a previous report indicating that permanent transfection of cyclin E, but not cyclin D1, induces aneuploidy in cultured cells (46). The discrepancy may be due to differences in transfection techniques, experimental conditions, or susceptibility of various cell types. Our finding that short-term cyclin D1 overexpression induced centrosome and mitotic spindle abnormalities in breast epithelial cells (Fig. 9) indicates that this effect is not limited to hepatocytes and could potentially affect

chromosome stability in different types of tumors with constitutive expression of this protein. Indeed, several reports have shown that cyclin D1 is associated with aneuploidy in a variety of malignant cell types (15-18), which is consistent with the notion that persistent expression of this protein promotes mitotic abnormalities in human malignancies.

The mice transiently transfected with cyclin D1 mice did not develop overt signs of malignancy during the relatively short period of observation. However, this was not formally addressed because we did not sustain a large number of animals over a longer period. The striking mitotic abnormalities seen 6 days after cyclin D1 transfection were associated with substantial hepatocyte apoptosis as well as induction of p53 and p21 in these livers. Previous studies in p53 and p21 knockout cells indicate that these proteins play an important role in preventing centrosome abnormalities, presumably by activating checkpoint mechanisms and inhibiting cdk2, respectively (10). In our studies, centrosome and chromosome abnormalities apparently induced checkpoint mechanisms that promoted apoptosis and cell cycle arrest, which effectively removed the most aberrant cells. Interestingly, we did note that a proportion of cells demonstrated increased numbers of centrosomes 4 months after cyclin D1 transfection. Since the first-generation adenovirus system produces transgene expression that lasts only weeks (20,24), these results indicate that some of the centrosome changes induced by cyclin D1 overexpression may persist even when the protein is no longer expressed. In the setting of persistent hepatocyte proliferation or mutations of p53 gene (which are commonly observed in hepatocellular carcinoma (HCC) (41,47,48)), these cyclin D1-induced

centrosome changes could play a potentially important role in the development of aneuploidy.

In humans, HCC occurs almost exclusively in the setting of longstanding chronic liver diseases, which generally demonstrate ongoing hepatocyte destruction and proliferation (41,48). Previous studies have found that a high level of hepatocyte proliferation observed on liver biopsy specimens correlates with an increased risk of HCC (49-51). Both HCC and preneoplastic foci of dysplastic hepatocytes are characterized by widespread and heterogeneous chromosome changes (41,47). Although it is absent in normal adult liver, cyclin D1 is upregulated following liver injury in diverse animal models and is expressed in human liver demonstrating evidence of hepatocyte replication (31). Clinical HCC specimens with high-level cyclin D1 expression were found to have a highly dysplastic morphologic phenotype (52), although the relationship of cyclin D1 expression and chromosome abnormalities has not been formally evaluated in this cancer (to our knowledge). The current study suggests that persistent cyclin D1 expression – induced by chronic mitogenic stimulation, oncogenic mutations of upstream signaling molecules, or chromosome rearrangements involving the *cyclin D1* gene – could potentially contribute to the striking and apparently random chromosome abnormalities seen in many HCCs (41,47).

These findings should raise a note of caution regarding recombinant adenoviruses, which have been used extensively to achieve high-efficiency transient transfection in culture and *in vivo* (24). These vectors readily transfect hepatocytes in the liver after intravenous injection, and can target genes to other organs as well (24). Recombinant adenoviruses expressing cyclin D1 trigger proliferation of quiescent hepatocytes and

cardiomyocytes *in vivo*, suggesting a possible strategy to promote adaptive parenchymal cell replication in disease states (20,53). The carcinogenic potential of adenoviral vectors has been thought to be minimal since they do not insert into the chromosome DNA. NIH Guidelines suggest that Biosafety Level II containment measures are sufficient for recombinant adenoviruses.[1] However, our findings indicate that even short-term overexpression of cyclin D1 produces chromosome instability. Thus, strategies to transiently transfect cyclin D1 (and conceivably other growth-promoting genes) could induce unanticipated genetic alterations even if the vectors do not integrate into cellular DNA. More stringent laboratory containment procedures for viral vectors encoding potential oncogenes may therefore be advisable.

The results presented here indicate that aberrant cyclin D1 expression rapidly induces alterations of the mitotic apparatus and aneuploidy in normal cells. We believe that these studies provide the most direct evidence to date that overexpression of cyclin D1 alone can lead to genomic instability. Furthermore, our short-term experiments showed that under these conditions, centrosome duplication was not proportional to DNA replication, suggesting that the centrosome cycle and the cell cycle can be uncoupled. Cyclin D1 should therefore be added to the list of cancer-related genes that regulate centrosome duplication and the mitotic spindle apparatus (5). The induction of chromosome instability by cyclin D1 could play an important role in the carcinogenic effect of this oncogene.

Acknowledgements – We thank Julie Bune and David Rickheim for excellent technical assistance, Linda M. Sargent for advice on mouse hepatocyte chromosome analysis, and Jeffrey Salisbury for centrin antibodies.

Footnotes

[1]Abbreviations: ADV, recombinant adenovirus; cdk, cyclin-dependent kinase; HCC, hepatocellular carcinoma; RT-PCR, real-time polymerase chain reaction.

[2]http://www4.od.nih.gov/oba/rac/guidelines_02/NIH_Guidelines_Apr_02.htm

References

1. Rajagopalan, H., Nowak, M. A., Vogelstein, B., and Lengauer, C. (2003) *Nat Rev Cancer* **3**, 695-701
2. Sen, S. (2000) *Curr Opin Oncol* **12**, 82-88
3. Salisbury, J. L., Whitehead, C. M., Lingle, W. L., and Barrett, S. L. (1999) *Biol Cell* **91**, 451-460.
4. Brinkley, B. R. (2001) *Trends Cell Biol* **11**, 18-21.
5. Nigg, E. A. (2002) *Nat Rev Cancer* **2**, 815-825
6. Lingle, W. L., Barrett, S. L., Negron, V. C., D'Assoro, A. B., Boeneman, K., Liu, W., Whitehead, C. M., Reynolds, C., and Salisbury, J. L. (2002) *Proc Natl Acad Sci U S A* **99**, 1978-1983.
7. Lange, B. M. (2002) *Curr Opin Cell Biol* **14**, 35-43.
8. Hinchcliffe, E. H., and Sluder, G. (2001) *Genes Dev* **15**, 1167-1181.
9. Hinchcliffe, E. H., and Sluder, G. (2001) *Curr Biol* **11**, R698-701.
10. Tarapore, P., and Fukasawa, K. (2002) *Oncogene* **21**, 6234-6240
11. Warner, S. L., Bearss, D. J., Han, H., and Von Hoff, D. D. (2003) *Mol Cancer Ther* **2**, 589-595
12. Malumbres, M., and Barbacid, M. (2001) *Nature Rev Cancer* **1**, 222-231.
13. Bartek, J., and Lukas, J. (2001) *Nature* **411**, 1001-1002
14. Sherr, C. J. (2000) *Cancer Res* **60**, 3689-3695.
15. Collecchi, P., Santoni, T., Gnesi, E., Giuseppe Naccarato, A., Passoni, A., Rocchetta, M., Danesi, R., and Bevilacqua, G. (2000) *Cytometry* **42**, 254-260.
16. Lung, J. C., Chu, J. S., Yu, J. C., Yue, C. T., Lo, Y. L., Shen, C. Y., and Wu, C. W. (2002) *Genes Chromosomes Cancer* **34**, 276-284.
17. Ott, G., Kalla, J., Ott, M. M., Schryen, B., Katzenberger, T., Muller, J. G., and Muller-Hermelink, H. K. (1997) *Blood* **89**, 1421-1429
18. Rennstam, K., Baldetorp, B., Kytola, S., Tanner, M., and Isola, J. (2001) *Cancer Res* **61**, 1214-1219
19. Nelsen, C. J., Hansen, L. K., Rickheim, D. G., Chen, C., Stanley, M. K., Krek, W., and Albrecht, J. H. (2001) *Oncogene* **20**, 1825-1831
20. Nelsen, C. J., Rickheim, D. G., Timchenko, N. A., Stanley, M. W., and Albrecht, J. H. (2001) *Cancer Res* **61**, 8564-8568.
21. Nelsen, C. J., Rickheim, D. G., Tucker, M. M., Hansen, L. K., and Albrecht, J. H. (2003) *J Biol Chem* **278**, 3656-3663
22. Nelsen, C. J., Rickheim, D. G., Tucker, M. M., McKenzie, T. J., Hansen, L. K., Pestell, R. G., and Albrecht, J. H. (2003) *J Biol Chem* **278**, 25853-25858
23. Albrecht, J. H., and Hansen, L. K. (1999) *Cell Growth Differ* **10**, 397-404
24. Becker, T. C., Noel, R. J., Coats, W. S., Gomez-Foix, A. M., Alam, T., Gerard, R. D., and Newgard, C. B. (1994) *Methods Cell Biol* **43**, 161-189
25. Kuriyama, R., Ohta, T., Vogel, J., and Peng, G. (2001) *Methods Cell Biol* **67**, 125-140
26. Ohta, T., Essner, R., Ryu, J. H., Palazzo, R. E., Uetake, Y., and Kuriyama, R. (2002) *J Cell Biol* **156**, 87-99.

27. D'Assoro, A. B., Barrett, S. L., Folk, C., Negron, V. C., Boeneman, K., Busby, R., Whitehead, C., Stivala, F., Lingle, W. L., and Salisbury, J. L. (2002) *Breast Cancer Res Treat* **75**, 25-34
28. Albrecht, J. H., Poon, R. Y., Ahonen, C. L., Rieland, B. M., Deng, C., and Crary, G. S. (1998) *Oncogene* **16**, 2141-2150
29. Loyer, P., Cariou, S., Glaise, D., Bilodeau, M., Baffet, G., and Guguen-Guillouzo, C. (1996) *J Biol Chem* **271**, 11484-11492
30. Hansen, L. K., and Albrecht, J. H. (1999) *J Cell Sci* **112**, 2971-2981
31. Fausto, N., and Campbell, J. S. (2003) *Mech Dev* **120**, 117-130.
32. Michalopoulos, G. K., and DeFrances, M. C. (1997) *Science* **276**, 60-66
33. Kozarsky, K. F., Donahee, M. H., Rigotti, A., Iqbal, S. N., Edelman, E. R., and Krieger, M. (1997) *Nature* **387**, 414-417
34. Ilan, Y., Saito, H., Thummala, N. R., and Chowdhury, N. R. (1999) *Semin Liver Dis* **19**, 49-59
35. Iimuro, Y., Nishiura, T., Hellerbrand, C., Behrns, K. E., Schoonhoven, R., Grisham, J. W., and Brenner, D. A. (1998) *J Clin Invest* **101**, 802-811
36. Lingle, W. L., and Salisbury, J. L. (2001) *Methods Cell Biol* **67**, 325-336
37. Guidotti, J. E., Bregerie, O., Robert, A., Debey, P., Brechot, C., and Desdouets, C. (2003) *J Biol Chem* **278**, 19095-19101
38. Meraldi, P., Honda, R., and Nigg, E. A. (2002) *Embo J* **21**, 483-492.
39. Sutherland, R. L., and Musgrove, E. A. (2002) *Breast Cancer Res* **4**, 14-17
40. Deane, N. G., Parker, M. A., Aramandla, R., Diehl, L., Lee, W. J., Washington, M. K., Nanney, L. B., Shyr, Y., and Beauchamp, R. D. (2001) *Cancer Res* **61**, 5389-5395.
41. Grisham, J. W. (2004) in *Gastrointestinal Oncology* (Abbruzzese, J. L., Evans, D. B., Willett, C. G., and Fenoglio-Preiser, C., eds), pp. 471-506, Oxford University Press, New York
42. Hahn, W. C., and Weinberg, R. A. (2002) *Nat Rev Cancer* **2**, 331-341
43. Coqueret, O. (2002) *Gene* **299**, 35-55
44. Duesberg, P., Li, R., and Rasnick, D. (2004) *Cell Cycle* **3**, 823-828
45. Rickheim, D. G., Nelsen, C. J., Fassett, J. T., Timchenko, N. A., Hansen, L. K., and Albrecht, J. H. (2002) *Hepatology* **36**, 30-38.
46. Spruck, C. H., Won, K. A., and Reed, S. I. (1999) *Nature* **401**, 297-300
47. Thorgeirsson, S. S., and Grisham, J. W. (2002) *Nat Genet* **31**, 339-346
48. Levy, L., Renard, C. A., Wei, Y., and Buendia, M. A. (2002) *Ann N Y Acad Sci* **963**, 21-36.
49. Tarao, K., Shimizu, A., Ohkawa, S., Harada, M., Ito, Y., Tamai, S., Kuni, Y., Okamoto, N., Inoue, T., and Kanisawa, M. (1992) *Gastroenterology* **103**, 595-600
50. Tarao, K., Ohkawa, S., Shimizu, A., Harada, M., Nakamura, Y., Ito, Y., Tamai, S., Hoshino, H., Inoue, T., and Kanisawa, M. (1994) *Cancer* **73**, 1149-1154
51. Shibata, M., Morizane, T., Uchida, T., Yamagami, T., Onozuka, Y., Nakano, M., Mitamura, K., and Ueno, Y. (1998) *Lancet* **351**, 1773-1777
52. Ito, Y., Matsuura, N., Sakon, M., Miyoshi, E., Noda, K., Takeda, T., Umeshita, K., Nagano, H., Nakamori, S., Dono, K., Tsujimoto, M., Nakahara, M., Nakao, K., Taniguchi, N., and Monden, M. (1999) *Hepatology* **30**, 90-99

53. Tamamori-Adachi, M., Ito, H., Sumrejkanchanakij, P., Adachi, S., Hiroe, M., Shimizu, M., Kawauchi, J., Sunamori, M., Marumo, F., Kitajima, S., and Ikeda, M. A. (2003) *Circ Res* **92**, e12-19

Figure Legends

Figure 1. Cyclin D1 induces abnormal hepatocyte mitoses *in vivo.* BALB/c mice were transfected by intravenous injection of a recombinant adenovirus expressing human cyclin D1. Hematoxylin and eosin-stained liver biopsy specimens obtained 2 and 6 days after transfection were evaluated by routine microscopy.

Figure 2. Induction of supernumerary centrosomes and abnormal mitotic spindle formation by cyclin D1. Hepatocytes were transfected *in vivo* with the cyclin D1 (ADV-D1), cyclin E (ADV-E) or control adenoviruses for 3 days. Hepatocytes were then isolated, placed in culture for 2 days, and fixed for immunohistochemistry or FACS analysis. Cells used for histology were treated with colchemid for the final 3 hours of culture. Normal cells were isolated and cultured in parallel without transfection. (**A**) Centrosome and mitotic spindle morphology. Cells were immunostained with antibodies to Cep-135 (red) and α-tubulin (green). The *inset* shows multiple Cep135-staining centrosomes at a single spindle pole in a cyclin D1-transfected cell. In the merged picture, Cep135-positive foci appear yellow. (**B**) Centrosome number per mitotic cell in normal, control-transfected, cyclin E-transfected, and cyclin D1-transfected hepatocytes (3-4 animals per group). (**C**) Centriole staining. Hepatocytes were co-immunostained for centrin (green) and Cep-135 (red) and photographed under high power magnification. (**D**) FACS analysis of propidium iodide-stained hepatocytes. A portion of cyclin D1-transfected cells exhibited DNA contents that did fall into the major 2N, 4N, and 8N peaks. (**E**) The percentage of DAPI-stained cells displaying metaphase morphology under each condition.

Figure 3. Centrosome overduplication in interphase cells following cyclin D1 transfection. (**A**) Hepatocytes were transfected with ADV-D1, cultured, and stained with Cep-135 (red) and α-tubulin (green) as in Fig. 2. A representative cell is shown, displaying distinct centrosomes grouped together in one region. (**B**) Centrosome number per interphase cell following cyclin D1 transfection.

Figure 4. Centrosome and mitotic spindle morphology at an early time point. Hepatocytes were transfected for 1 day *in vivo*, placed in culture for 1 day, and analyzed as in Fig. 2. (**A**) Immunostaining for Cep135 (red) and α-tubulin (green). The *inset* shows multiple centrosomes clustering at a single spindle pole. (**B**) Centrosome number per mitotic cell. (**C**) FACS analysis.

Figure 5. Destabilization of chromosomes by cyclin D1. Hepatocytes were transfected and harvested as in Fig. 2. After fixation, mitotic spreads were prepared and stained with Giemsa as described in Experimental Procedures. (**A**) Chromosome number per cell. A total of 50 mitotic spreads were analyzed for each condition. (**B**) Representative micrographs of chromosome abnormalities in cyclin D1-transfected cells.
(**C**) Quantification of the number of chromosome abnormalities per mitotic cell.

Figure 6. Induction of hepatocyte apoptosis by cyclin D1 *in vivo*. Liver sections obtained at 1 and 6 days after transfection with the control or cyclin D1 adenovirus were subjected to TUNEL staining. The percentage of TUNEL-positive cells is shown at each time point.

Figure 7. Upregulation of p53 and p21 mRNA expression cyclin D1. RNA was extracted from cyclin D1- or control-transfected livers at 1 and 6 days. Expression of p53 and p21 mRNA were quantified by RT-PCR and normalized to β-actin mRNA as described in Experimental Procedures.

Figure 8. Residual centrosome abnormalities 4 months after cyclin D1 transfection. Hepatocytes were isolated from mice 4 months after transfection with the cyclin D1 or control adenoviruses, placed in culture for 3 days, and immunostained for Cep-135 as in Fig. 2. Hepatocytes were also isolated from age-equivalent untransfected normal mice. The number of centrosomes per mitotic cell is shown.

Figure 9. Short-term cyclin D1 transfection induces centrosome abnormalities in breast epithelial cells. Cultured human breast epithelial cells were transfected with the control or cyclin D1 adenoviruses for 2 days as described in Experimental Procedures. Fixed cells were immunostained with α-tubulin (green) or γ-tubulin (red). In the merged image, co-localization of α- and γ-tubulin results in yellow fluorescence. Control-transfected cells did not demonstrate any differences relative to normal untransfected cells (data not shown).

file02.tif

Figure 1

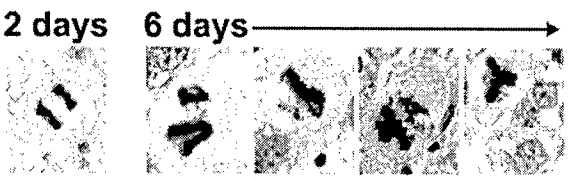

Figure 2

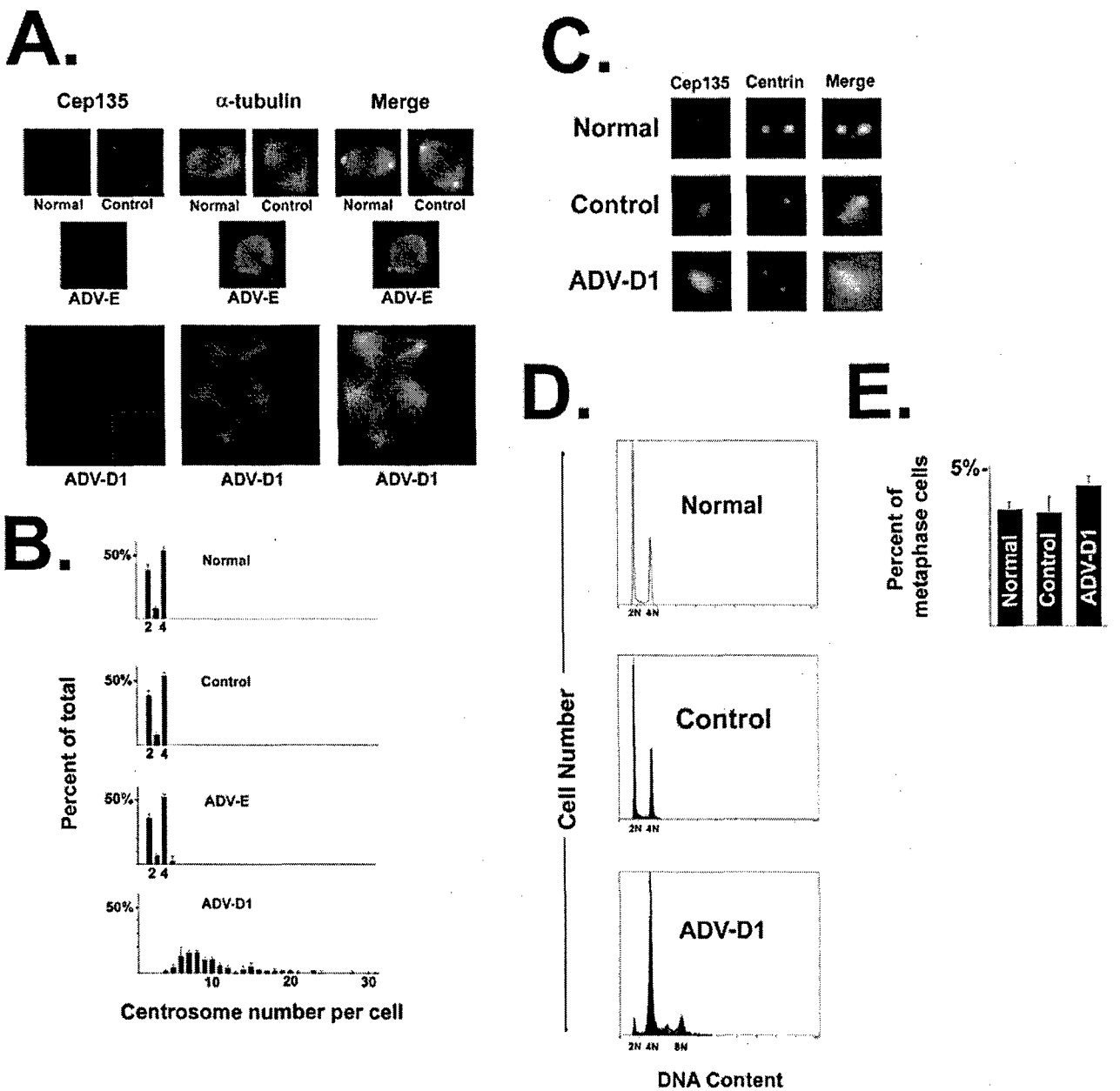
A.
Cep135
α-tubulin
Merge
Normal
Control
ADV-E
ADV-D1
B.
50%
Normal
Control
ADV-E
ADV-D1
2 4
10
20
30
Percent of total
Centrosome number per cell
C.
Cep135
Centrin
Merge
Normal
Control
ADV-D1
D.
Normal
Control
ADV-D1
2N 4N
2N 4N 8N
Cell Number
DNA Content
E.
Percent of metaphase cells
5%
Normal
Control
ADV-D1

Figure 3

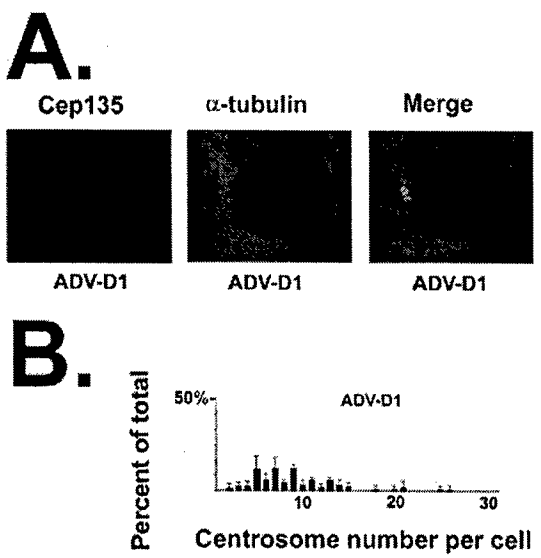
A.
Cep135
α-tubulin
Merge
ADV-D1
ADV-D1
ADV-D1
B.
Percent of total
50%
ADV-D1
10
20
30
Centrosome number per cell

Figure 4

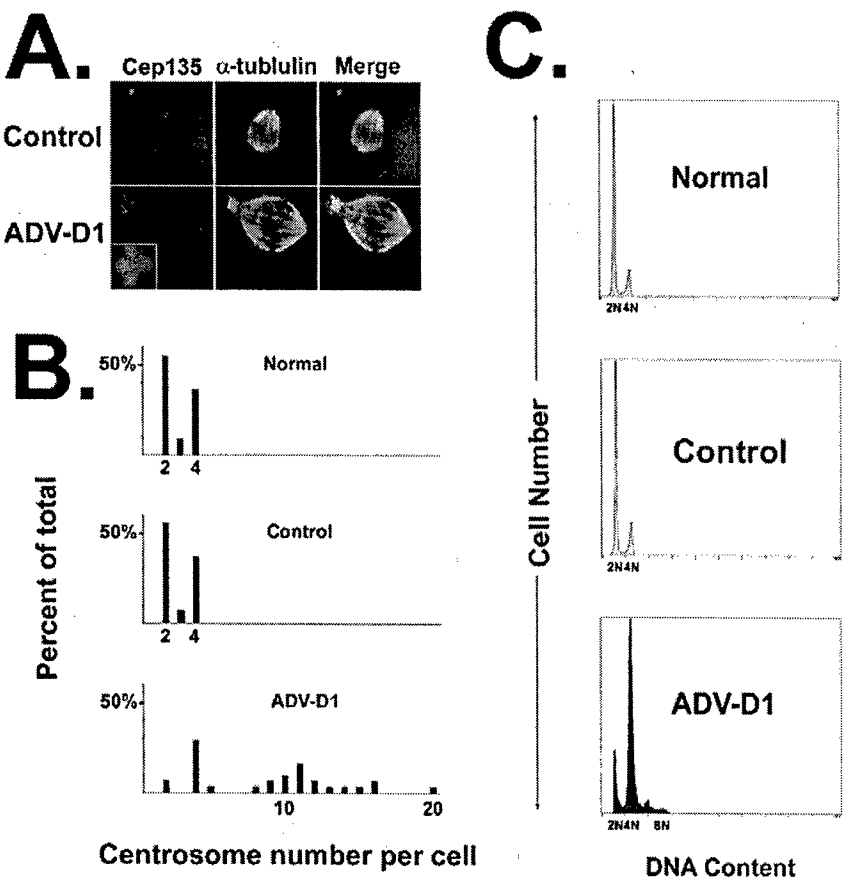
A.
Cep135
α-tublulin
Merge
Control
ADV-D1
B.
50%
Normal
2
4
50%
Control
2
4
50%
ADV-D1
10
20
Percent of total
Centrosome number per cell
C.
Normal
2N4N
Control
2N4N
ADV-D1
2N4N
8N
Cell Number
DNA Content

Figure 5

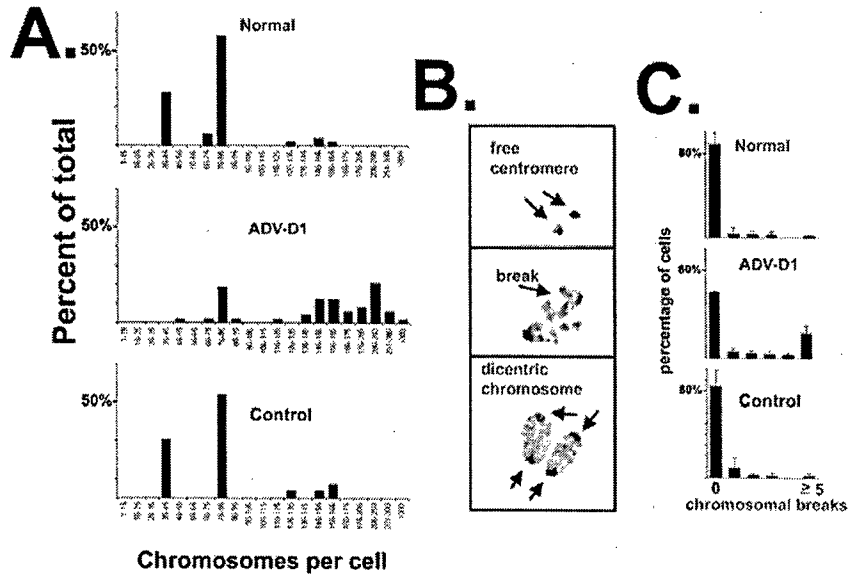
A.
Normal
50%
ADV-D1
50%
Control
50%
Percent of total
Chromosomes per cell
B.
free centromere
break
dicentric chromosome
C.
Normal
80%
ADV-D1
80%
Control
80%
percentage of cells
0
≥ 5
chromosomal breaks

Figure 6

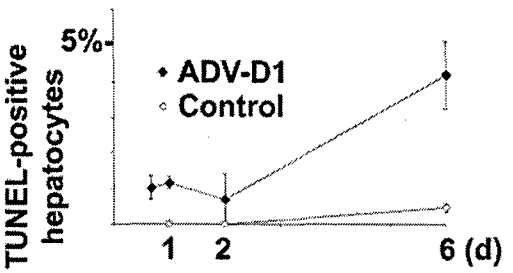

Figure 7

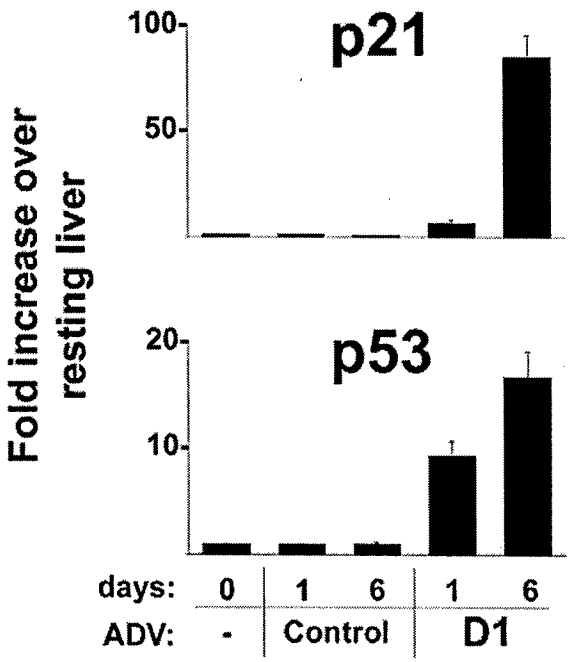
p21
100
50
p53
20
10
Fold increase over resting liver
days: 0 1 6 1 6
ADV: - Control D1

Figure 8

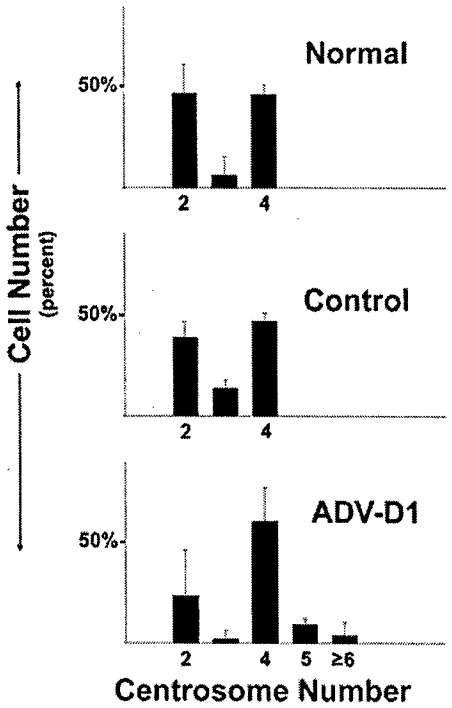
Normal
50%
2
4
Control
50%
2
4
ADV-D1
50%
2
4
5
≥6
Cell Number
(percent)
Centrosome Number

Figure 9